Immunological correlates of protection following vaccination with glucan particles containing Cryptococcus neoformans chitin deacetylases

Stuart Levitz (Stuart.Levitz@umassmed.edu)
University of Massachusetts Chan Medical School https://orcid.org/0000-0002-3799-3064
Ruiying Wang (ruiying.wang@umassmed.edu)
University of Massachusetts Medical School https://orcid.org/0000-0002-3638-4582
Lorena Oliveira (lorena.ramalho@umassmed.edu)
University of Massachusetts Medical School https://orcid.org/0000-0002-1762-0076
Diana Lourenco (diana.lourenco@umassmed.edu)
University of Massachusetts Chan Medical School
Christina Gomez (christina.gomez@abbvie.com)
University of Massachusetts Chan Medical School
Chrono Lee (Chrono.Lee@umassmed.edu)
University of Massachusetts Chan Medical School
Maureen Hester (maureen.hester@umassmed.edu)
University of Massachusetts Chan Medical School
Zhongming Mou (umass_08@yahoo.com)
University of Massachusetts Chan Medical School
Gary Ostroff (gary.ostroff@umassmed.edu)
University of Massachusetts Chan Medical School
Charles Specht (charles.specht@umassmed.edu)
University of Massachusetts Medical School https://orcid.org/0000-0002-5749-3112

Article

Keywords:

DOI: https://doi.org/

Additional Declarations: (Not answered)

Immunological correlates of protection following vaccination with glucan particles containing *Cryptococcus neoformans* chitin deacetylases

Running title: Cryptococcus vaccination and immune correlates of protection

Ruiying Wang[1#], Lorena V.N. Oliveira[1#], Diana Lourenco[1], Christina L. Gomez[1], Chrono K. Lee[1], Maureen M. Hester[1], Zhongming Mou[1], Gary R. Ostroff[2], Charles A. Specht[1*], and Stuart M. Levitz[1*]

1 Department of Medicine, The University of Massachusetts Chan Medical School, Worcester, MA, United States

2 Program in Molecular Medicine, The University of Massachusetts Chan Medical School, Worcester, MA, United States

[#] Drs. Wang and Oliveira contributed equally to this work.

* Drs. Specht and Levitz share senior authorship.

Corresponding Authors:

Stuart M. Levitz, M.D.

stuart.levitz@umassmed.edu

Department of Medicine, LRB317

UMass Chan Medical School

Worcester, MA 01605

Charles A. Specht

charles.specht@umassmed.edu

Department of Medicine, LRB370D

UMass Chan Medical School

Worcester, MA 01605

ABSTRACT

Vaccination with glucan particles (GP) containing the *Cryptococcus neoformans* chitin deacetylases Cda1 and Cda2 protect mice against experimental cryptococcosis. Here, immunological correlates of vaccine-mediated protection were explored. Studies comparing knockout and wild-type mice demonstrated $CD4^+$ T cells are crucial, while B cells and $CD8^+$ T cells are dispensable. Protection was abolished following $CD4^+$ T cell depletion during either vaccination or infection, but was retained if $CD4^+$ T cells were only partially depleted. Vaccination elicited systemic and durable antigen-specific immune responses in PBMCs, spleen and lungs. Following vaccination and fungal challenge, robust Th1 and Th17 responses were observed in the lungs. Protection was abrogated in mice congenitally deficient in IFNɣ, IFNɣ receptor, IL-1β, IL-6, or IL-23. Thus, $CD4^+$ T cells and specific pro-inflammatory cytokines are required for GP-vaccine mediated protection. Importantly, retention of protection in the setting of partial $CD4^+$ T depletion suggests a pathway for vaccinating at-risk immunocompromised individuals.

INTRODUCTION

Cryptococcosis is an invasive fungal infection caused by fungi of the genus *Cryptococcus*, mainly *C. neoformans* and *C. gattii*. Exposure is thought to most commonly occur following inhalation of aerosolized cells from the environment. In most persons, host defenses are sufficient to kill or contain the fungus in a latent state. However, in susceptible hosts, pneumonia, and life-threatening disseminated infection, especially to the central nervous system can occur[1]. Persons with advanced HIV disease are most vulnerable; however, other immunocompromised individuals with impaired $CD4^+$ T cell defenses are also at higher risk, including patients with hematological malignancies, and those on immunosuppressing medications to treat autoimmune conditions, or to prevent rejection following solid organ transplantation[2]. The global burden of HIV-associated cryptococcal meningitis in 2020 was estimated at 152,000 cases, including 112,000 deaths[3].

Although the incidence and mortality of HIV-associated cryptococcal meningitis have declined in high-income countries, it remains a major health issue in resource-limited areas that have a high prevalence of HIV coupled with insufficient access to diagnostic testing, antiretroviral treatment, and antifungal drugs[2]. Regardless of the setting, once cryptococcal meningitis develops, even with currently available treatments, the morbidity and mortality are substantial[2,4]. Thus, preventative measures, such as the development of efficacious vaccines are urgently needed. However, no licensed anti-cryptococcal vaccine is available for use[5].

One approach to cryptococcal vaccine development is the use of whole organism vaccines that are attenuated by deletion of virulence factors, such as the capsular polysaccharide glucuronoxylomannan, cell wall chitosan, sterylglucosidase, and F-box protein[5-9]. Another approach is engineering *C. neoformans* strains, so they express heterologous murine interferon (IFN)-γ or overexpress zinc finger protein[10-12]. Whole organism vaccines are relatively easy to manufacture and generally induce good immune responses. Drawbacks, however, include the

potential for reactogenicity, autoimmunity, and for live vaccines, infection. Therefore, we have focused on identifying *C. neoformans* protein antigens which can be used in subunit vaccines. Two of the most promising vaccine antigens, Cda1 and Cda2, are members of the chitin deacetylase (Cda) family with no significant homology to human proteins. This, plus their strong immunogenicity and role in catalyzing the deacetylation of chitin to the virulence determinant chitosan make them attractive candidate vaccine antigens[13]. We have demonstrated that glucan particle (GP)-based subunit vaccines, including GP-Cda1 and GP-Cda2 (alone and in combination), could afford a significant survival advantage following pulmonary challenge of mice with the highly virulent *C. neoformans* KN99 strain[14-16]. Some survivors even had undetectable colony forming units (CFUs) in the lungs at the termination of the experiment.

Here we probed the immunological correlates of GP vaccine-mediated protection by examining mice with congenital and acquired deficiencies in specific aspects of immune function. We demonstrate CD4+T cells and certain cytokines are crucial for GP-Cda1 and GP-Cda2 vaccine-induced immunity. Furthermore, we investigated the nature of the antigen-specific immune response by *ex vivo* restimulation of peripheral blood mononuclear cells (PBMC), splenocytes, and lung leukocytes from wild type (WT) mice that were vaccinated and/or infected. Systemic and durable immune responses were observed in the vaccinated and infected mice, with a robust T-helper (Th) 1 and Th17 response detected in the lung.

RESULTS

B cells are dispensable for GP-Cda1 or GP-Cda2 vaccine-mediated protection

In initial experiments, we examined the role of B cells in GP-Cda1 and GP-Cda2 vaccine-mediated protection from pulmonary cryptococcal challenge by comparing two mouse strains congenitally deficient in B cells to their WT counterparts. μMT mice, which have a C57BL/6 background, lack mature B cells and expression of membrane-bound IgM[17]. Following

pulmonary challenge with *C. neoformans*, survival of unvaccinated WT and μMT mice was similar, with all mice succumbing to infection by day 25 (Fig. 1A and 1B). Both GP-Cda1 and GP-Cda2 vaccination significantly protected the WT and μMT mice, with no statistically significant differences noted comparing the mouse strains. Similar results were seen comparing WT BALB/c mice with $Jh^{-/-}$ mice on the BALB/c background. $Jh^{-/-}$ mice carry a deletion of the endogenous murine J segments of the Ig heavy chain locus; as a consequence, they lack mature B cells and have no detectable antibody[18]. Unvaccinated $Jh^{-/-}$ mice succumbed to cryptococcosis by day 25, whereas the WT BALB/c all died by day 30. However, robust protection of $Jh^{-/-}$ mice and WT BALB/c mice was observed following vaccination with either GP-Cda1 or GP-Cda2 (Fig. 1C and 1D). Thus, vaccine-induced protection is not abrogated by B cell deficiency.

$CD4^+$ but not $CD8^+$ T cells are crucial for GP-Cda1 or GP-Cda2 vaccine-induced protection

We next investigated the contribution of T cell subsets to protection mediated by GP-Cda1 and GP-Cda2 vaccines. We first examined whether the $CD8^+$ T cell subset contributed to protection in $CD8^+$ T cell-deficient β-2-microglobulin knockout ($\beta2m^{-/-}$) mice. Unvaccinated WT and $\beta2m^{-/-}$ mice all died by 28 days post infection (dpi). However, protection was retained in the $\beta2m^{-/-}$ mice for both vaccines; if anything, there was a non-significant trend towards enhanced survival in the mutant mice (Fig. 2A and 2B).

Clinical and experimental studies demonstrate that $CD4^+$ T cells are critical for protective immunity against cryptococcosis[19]. Therefore, we next tested our GP-Cda1 and GP-Cda2 vaccines in $MHCII^{-/-}$ mice, which are devoid of all four classical murine MHC Class II chains and consequently lack $CD4^+$ T cells. Whether receiving GP-Cda1 or GP-Cda2 vaccination, mice lacking $CD4^+$ T cells had 100% mortality by 33 dpi, similar to that seen for unvaccinated mice (Fig. 2C and 2D). Thus, protection was lost in mice with $CD4^+$ T cell deficiency. As expected, protection was retained in the WT vaccinated mice.

GP-Cda2 vaccine-mediated protection requires CD4+ T cells during both the vaccination and challenge phases of the experiment

As an alternative approach to assess the importance of CD4+ T cells for vaccine-induced protection, we studied the effect on survival when the anti-CD4 monoclonal antibody GK1.5 was administered to GP-Cda2-vaccinated mice (Fig. 3). As shown in Fig. 4A, injection of 200 µg of GK1.5 led to nearly complete depletion of blood CD4+ T cells for two weeks. Two strategies for CD4+ T cell depletion were conducted. In the first, mice were depleted of CD4+ T cells in the vaccination phase by giving a dose of GK1.5 two days prior to each vaccination. For the second strategy, GK1.5 was given two days prior to fungal challenge and then two additional biweekly injections were given (Fig. 3A). Regardless of whether the GK1.5 was administered during the vaccination or the challenge phase, vaccine-mediated protection was completely lost (Fig. 3B). As expected, the vaccinated mice that did not get GK1.5 survived significantly longer than the unvaccinated mice.

Retention of GP-Cda1/Cda2 vaccine-mediated protection despite partial CD4+ T cell depletion

The data shown in Figures 2 and 3 demonstrate loss of vaccine-mediated protection in the setting of complete CD4+ T cell deficiency. However, populations at risk for cryptococcosis generally are only partially deficient in CD4+ T cell function. For example, most HIV-positive persons have blood CD4+ T cell counts above 100 cells/µL when they are initially found to be HIV-infected or following initiation of antiretroviral therapy[20]. To model whether a vaccine could potentially protect this immunocompromised population, we evaluated doses of anti-CD4 Ab GK1.5 that result in only partial depletion of CD4+ T cells. First, using naïve BALB/c mice, we performed a dose-response experiment to determine the kinetics of blood CD4+ T cell counts following administration of GK1.5 (Fig. 4A). Following a single injection of 200 µg GK1.5, CD4+ T cells were nearly completely depleted in the blood for two weeks and then gradually increased

at subsequent time points. The dose of 40 µg also resulted in profound depletion of $CD4^+$ T cells but counts began to recover after one week. Depletion was also seen using the 8 µg and 1.6 µg doses, but the diminution in $CD4^+$ T cell counts were more modest. For all doses of GK1.5 tested, $CD4^+$ T cell counts never recovered to levels seen in untreated mice.

Next, we immunized mice with the two-antigen combination GP-Cda1/Cda2 vaccine. Two days prior to cryptococcal challenge, mice were partially depleted of their $CD4^+$ T cells using the range of doses tested in Fig. 4A. Mice were then followed over 70 days for survival. Vaccine-mediated protection was inversely proportional to the GK1.5 dose (Fig. 4B). Importantly, all groups of vaccinated mice that received ≤40 µg GK1.5 had ≥50% survival at the end of the study. Taken together with the data in Fig. 3, our results suggest vaccine efficacy is retained in the setting of modest, but not severe, $CD4^+$ T cell immunocompromise.

GP-Cda1/Cda2 vaccination induces systemic and durable antigen-specific immune responses

For the next two sets of experiments (Fig. 5 and 6), we sought to determine the nature of the adaptive immune response to vaccination and infection. To do so, *ex vivo* antigen-stimulated responses were investigated in five groups of BALB/c mice: 1) unvaccinated, unchallenged; 2) vaccinated, unchallenged; 3) unvaccinated, challenged, euthanized 10 dpi; 4) vaccinated, challenged, euthanized 10 dpi; 5) vaccinated, challenged, and euthanized 70 dpi. The vaccine administered was the GP-Cda1/Cda2 combination. The *ex vivo* antigenic stimuli consisted of purified Cda1 or Cda2 protein produced in *E. coli*, and heat-killed *C. neoformans*. Control cells were left unstimulated.

The first set of experiments measured IFNɣ secretion by antigen-stimulated PBMCs (Fig. 5A), splenocytes (Fig. 5B), and lung leukocytes (Fig. 5C) harvested from the five groups of mice. This cytokine was chosen as it is thought to be crucial for clearance and control of mouse and

human cryptococcal infection[21,22]. When comparing cells from the three anatomical sites, similar qualitative patterns of IFNɣ release were seen. As expected, antigen-stimulated cells from the naïve mice had low to undetectable levels of IFNɣ production. Cells from vaccinated but uninfected mice, obtained two weeks following the third vaccination, had remarkable IFNɣ secretion following *ex vivo* stimulation with the vaccine antigens, Cda1 and Cda2. In contrast, IFNɣ release following stimulation with heat-killed (HK) *C. neoformans* was much lower. When considering cells from mice that were infected but not vaccinated, Cda1 and Cda2 stimulated modest amounts of IFNɣ that were considerably lower than what were observed in the vaccinated group. For cells from mice that had been vaccinated and then harvested at 10 dpi, the recall immune response to Cda1 and Cda2 was similar to that seen in mice that had been only vaccinated. However, when stimulated with HK *C. neoformans*, PBMCs and lung cells had more robust IFNɣ release compared with the corresponding cells from the vaccination only group. Finally, of the five mice in the vaccinated group followed for 70 days after infection, all were alive with undetectable lung CFUs (Fig. 6A) at the termination of the study. Nevertheless, recall immune responses persisted in cells from all three anatomical sites, albeit at lower levels in the PBMCs. Overall, these data indicate that GP-Cda1/Cda2 vaccine-induced immunity is systemic and long-lasting.

GP-Cda1/Cda2 vaccinated mice have robust antigen-specific Th1 and Th17 responses in the pulmonary compartment following cryptococcal challenge

As lungs are sites of initial infection after natural exposure to airborne *Cryptococcus* by inhalation, the immune response in the pulmonary compartment is crucial for vaccine-induced protection. Thus, we set up the second set of experiments and further analyzed the lungs from the same groups of mice described in Fig. 5. Fungal clearance, numbers of leukocytes, $CD4^+$ T cells and $CD8^+$ T cells, T cell activation, and *ex vivo* antigen-stimulated intracellular cytokine production were studied.

189 At 10 dpi, although not statistically significant, there was a trend toward better fungal control
190 in the lungs of vaccinated compared to unvaccinated mice (Fig. 6A). Notably, mice that survived
191 to the end of study had undetectable lung CFUs. In mice vaccinated and infected, a remarkable,
192 10-fold influx of leukocytes, including $CD4^+$ T cells, into the lung was observed at 10 dpi (Fig. 6B,
193 6C). At 70 dpi, numbers of leukocytes and $CD4^+$ T cells were similar to values seen in
194 uninfected mice. $CD8^+$ T cell numbers in the lung also increased in vaccinated mice at 10 dpi
195 compared with naïve or unvaccinated infected mice; however, the extent of the increase was
196 considerably more modest compared to that seen with $CD4^+$ T cells (Fig. 6D).

197 We next examined the profile of the $CD4^+$ T cell response in the lungs following
198 subcutaneous vaccination and pulmonary infection (Fig. 6E, 6F, 6G and 6H). The lungs of mice
199 that were vaccinated but not infected had a non-significant trend towards increased numbers of
200 antigen-stimulated $CD4^+$ T cells expressing the activation marker CD154, and the intracellular
201 cytokines IFNγ, interleukin (IL) -17, and tumor necrosis factor (TNF) α in comparison to
202 unstimulated cells. In the lungs of mice that were both vaccinated and infected, at 10 dpi there
203 were dramatic increases in numbers of $CD4^+$T cells expressing CD154, IFNγ, IL-17, or TNFα
204 after antigen stimulation, regardless of whether the antigen was Cda1, Cda2, or HK KN99.
205 These numbers decreased at 70 dpi to levels that were similar to those observed in vaccinated
206 but uninfected mice. Lung $CD8^+$ T cells producing IFNγ following *ex vivo* antigen stimulation
207 were also found in vaccinated mice 10d post infection, albeit in considerably lower numbers
208 compared to what was observed with $CD4^+$ T cells (Fig. 4SA). However, we did not detect
209 significant numbers of $CD8^+$ T cells producing IL-17 or TNFα after stimulation (Fig. 4SB and
210 4SC).

211 **Contribution of specific cytokines to protection mediated by GP-Cda1 and GP-Cda2**
212 **vaccination**

The intracellular cytokine data demonstrate the capacity of pulmonary T cells from vaccinated and infected mice to produce specific cytokines in response to antigenic stimulation but do not prove that these cytokines are essential to vaccine-mediated protection. Thus, in the final set of experiments, we explored GP-Cda1 and GP-Cda2 vaccine-induced protection in a panel of mice with genetic deficiencies in selected cytokines and a cytokine receptor implicated in host defenses against cryptococcosis. As the knockout mice were on the C57BL/6 background, WT C57BL/6 mice were used as controls. Consistent with our published data[16], WT C57BL/6 mice vaccinated with GP-Cda1 and GP-Cda2 were significantly protected from *C. neoformans* challenge (Fig. 7). Protection was completely or nearly completely lost in mice deficient in IFNɣ (Fig. 7A), IFNɣ receptor (IFNɣR; Fig. 7B), IL-6 (Fig. 7C) and IL-23 (Fig. 7D), regardless of whether the mice received the GP-Cda1 or GP-Cda2 vaccine. For vaccinated mice deficient in TNFα (Fig. 7E), the picture was more complicated. GP-Cda1 vaccination protected 30% of the TNFα$^{-/-}$ mice but GP-Cda2 vaccination did not elicit protection. Finally, IL-1β$^{-/-}$ mice (Fig. 7F) were significantly protected by both vaccines, although the GP-Cda1 vaccine protected the WT mice significantly better than the mutant mice.

DISCUSSION

The mechanisms by which a vaccine elicits protective responses against its target pathogen are important to decipher as this knowledge may help predict which populations are likely to benefit. This is especially true for vaccines designed to protect persons with immunocompromise; for such populations, an ideal vaccine would stimulate responses in the parts of the immune system that are relatively intact. For cryptococcosis, in the absence of vaccination, development of an adaptive CD4^{+} T cell response is critical for host defenses against natural and experimental infections[23,24]. However, other arms of the immune system, including B cells and CD8^{+} T cells have been shown to play supportive roles[25,26]. In the present

study, we systematically examined the immunological mechanisms by which GP-based vaccines containing Cda1 and Cda2 protect against experimental cryptococcosis in mice.

Evidence for the importance of antibody responses in protection against cryptococcosis includes mouse and human studies associating antibody responses and Fc receptor polymorphisms with risk for developing cryptococcal infections[27,28]. In addition, passive administration of monoclonal antibodies directed against the cryptococcal capsular polysaccharide, glucuronoxylomannan (GXM), or vaccination with GXM conjugated to a carrier protein, prolonged survival or reduced fungal burdens in some mouse models of cryptococcosis[29-31]. However, in our studies, protection against cryptococcosis mediated by the GP-Cda1 and GP-Cda2 vaccines was retained in two different B cell deficiency mouse stains: μMT mice on C57BL/6 background and $Jh^{-/-}$ mice on the BALB/c background. These data indicate that antibody responses are not essential for anticryptococcal immunity elicited by the two GP-vaccines studied here. Similarly, Aguirre et al. found that μMT mice and WT C57BL/6 mice had comparable susceptibility to cryptococcosis regardless of whether the mice had received a sublethal intratracheal immunization with a live *C. neoformans* strain[32]. In another study, protection mediated by an IFNγ-producing *C. neoformans* vaccine strain was retained in B cell deficient $CD19^{-/-}$ mice[33]. Thus, B cells appear to be dispensable for multiple cryptococcal vaccine candidates under development.

Similar to B cells, our data demonstrate that $CD8^+$ T cells are dispensable for GP-Cda1 and GP-Cda2 vaccine-mediated protection. Vaccinated $\beta2m^{-/-}$ mice, deficient in $CD8^+$ T cells, survived as well as the vaccinated WT mice following lethal challenge with *C. neoformans*. Although IFNγ-producing $CD8^+$ T cells (Tc1) were found in GP-Cda1/Cda2 vaccinated and infected mice lungs, their numbers were considerably lower compared with the numbers of infiltrating $CD4^+$ T cells. In contrast, studies using primary pulmonary infection models found that although not playing a dominant role, $CD8^+$ T cells contributed to protective immunity and

cryptococcal clearance by mediating cellular recruitment, synergizing with $CD4^+$ T cells, secreting inflammatory cytokines, and lysing *Cryptococcus*-laden phagocytes[34-36].

While B cells and $CD8^+$ T cells were not required, two lines of evidence demonstrate the non-redundant contribution that $CD4^+$ T cells make to GP-vaccine mediated protection. First, vaccination with GP-Cda1 and GP-Cda2 failed to protect $CD4^+$ T cell-deficient $MHCII^{-/-}$ mice against cryptococcal challenge. Second, vaccine-mediated protection was lost when mice were depleted of $CD4^+$ T cells using a monoclonal antibody targeting CD4. Notably, protection was abrogated regardless of whether the $CD4^+$ T cells were depleted at the time of vaccination or during infection. These results are in marked contrast to what was observed with an attenuated *Blastomyces dermatitidis* vaccine which protected $CD4^+$ T cell-deficient mice against blastomycosis and histoplasmosis by eliciting IL-17-producing $CD8^+$ T cells (Tc17)[37]. However, no compensatory effect of $CD8^+$ T cells was observed in GP-Cda1 or GP-Cda2 vaccinated CD4-deficient mice in our study, reflecting the non-essential role for $CD8^+$ T cells in this model.

As $CD4^+$ T cells are required for GP-vaccine mediated immunity, these findings raise the question of whether the immunocompromised populations most at risk for cryptococcosis could still benefit from the vaccine. Taking into consideration that most immunocompromised individuals are only partially deficient in $CD4^+$ T cell number or function[20,38], we established a partial CD4 deletion animal model using a range of doses of the anti-CD4 mAb, GK1.5. The protection elicited by the GP-Cda1/Cda2 combination vaccine was inversely correlated with GK1.5 dosage. Importantly, mice with very low levels of blood $CD4^+$ T cells at the time of challenge were protected. The translational significance of these findings remains speculative. It may be possible to vaccinate persons living with HIV while their $CD4^+$ T cells counts are relatively high, either at early diagnosis or after antiretroviral treatment. In a recent multicenter trial of patients with cryptococcal meningitis conducted in sub-Saharan Africa, 64% of trial participants had previously received antiretroviral therapy[39]. Other potential *Cryptococcus*

287 vaccine recipients include patients for whom immunosuppression is anticipated in the future,
288 such as individuals on solid organ transplant waiting lists. Finally, it is also worth noting that
289 many cases of cryptococcosis are thought to be due to reactivation of latent disease[40,41]. In
290 these individuals, vaccination could stimulate immune responses to eliminate latent
291 cryptococcal foci.

292 The durability and pattern of compartmentalization of vaccine-induced immunity are
293 dependent, at least in part, on the vaccine antigens, delivery system, and route of
294 administration[5,42,43]. To explore how adaptive immunity develops after GP-subunit vaccination
295 and pulmonary cryptococcal infection, IFNɣ secretion was measured following *ex-vivo* antigen
296 stimulation of immune cells from blood, spleen, and lung leukocytes. Robust antigen-specific
297 immune responses were detected in all compartments for vaccinated mice with or without
298 infection. Of note, the 70d survivors of vaccination and infection still had strong responses, thus
299 suggesting that GP-Cda vaccines elicit durable local and systemic immunity in the experimental
300 pulmonary infection models.

301 The $CD4^+$ T lymphocyte subsets Th1 and (to a lesser extent) Th17 have been associated
302 with protective responses to cryptococcal infection. Postulated mechanisms include activation
303 and recruitment of M1 macrophages, dendritic cell maturation, and stimulation of
304 proinflammatory cytokine and chemokine production[44-46]. We have demonstrated GP-based
305 vaccines elicit strong antigen-specific Th1- and Th17-biased responses in mice and rats[47-49].
306 Consistent with these observations, following GP-Cda1/Cda2 vaccination and infection, mouse
307 lungs had a robust influx of activated $CD4^+$ T cells that produced IFNɣ (Th1), IL-17 (Th17), and
308 TNFα following *ex vivo* antigen stimulation. Moreover, significantly enhanced IFNɣ
309 concentrations in *ex vivo* culture supernatants were detected by ELISA in mice both vaccinated
310 and challenged. These results indicate $CD4^+$ T cells are an important source of IFNɣ, although
311 the modest increase of Tc1 cells suggests a supplementary role for $CD8^+$ T cells. Interestingly,

for mice vaccinated but not infected, increased levels of IFNɣ were also observed following antigen stimulation. However, the numbers of Th1 and Tc1 cells were not elevated to the degree seen with vaccinated and infected mice, thus suggesting the contribution of other cellular sources of IFNɣ, such as ILC1 cells, NK cells, B cells, macrophages, and dendritic cells[50].

Regardless of the cellular source, IFNγ was required for GP-Cda1- and GP-Cda2-induced protection from cryptococcal challenge, as evidenced by the near total loss of protection in mice genetically deficient in this cytokine or its receptor, IFNγR. Survival curves similar to those seen in unvaccinated mice were also observed in mice null for IL-6 and IL-23. These two cytokines have a myriad of immune functions including promoting Th17 development and are required for optimal host defenses against cryptococcosis[51-54]. For the other two cytokine knockout mice we studied, TNFα$^{-/-}$ and IL-1β$^{-/-}$, more complex phenotypes were seen with results depending upon the vaccine tested. The GP-Cda1 vaccine partially protected TNFα$^{-/-}$ and IL-1β$^{-/-}$ mice, with survival intermediate between that seen in unvaccinated and vaccinated WT mice. For the GP-Cda2 vaccine, protection was largely lost in the TNFα$^{-/-}$ mice, but similar to WT survival curves in the IL-1β$^{-/-}$ mice. The differential protection observed in the knockout mice when comparing the two vaccines raises the possibility that the vaccines activate different intracellular pathways. TNFα is produced following phagocytosis of *C. neoformans* and is thought to have a central role in host defenses against cryptococcosis[21,55]. IL-1β is released by mononuclear phagocytes, including dendritic cells, following activation of both the canonical NLRP3–ASC–caspase-1 inflammasome and the non-canonical NLRP3-ASC-caspase-8 inflammasome[56].

In summary, our preclinical studies illuminate the arms of the immune system which are required for GP-Cda1 and GP-Cda2 vaccines to protect mice from cryptococcosis. Using models of congenital and acquired deficiency, a crucial, non-redundant role was found for CD4$^+$ T cells. Moreover, vaccinated and infected mice had a robust pulmonary influx of CD4$^+$ T cells

expressing IFNɣ, IL-17, and TNFα. Mice deficient in these cytokines or in pathways leading to their production or responsiveness were no longer protected by vaccination. A major challenge will be bringing vaccines to the human populations most in need. Our discovery that mice are still protected in the setting of partial $CD4^+$ T cell depletion provides encouragement that GP-vaccines could still be employed in some immunodeficient hosts. However, to maximize protection in hosts with $CD4^+$ T cell impairment, it may be necessary to stimulate other arms of the immune system. One such strategy which we are exploring is studying whether vaccines containing cryptococcal protein antigens which are exposed on the capsular surface will stimulate protective opsonophagocytic antibody responses.

METHODS

Chemicals and Reagents

Chemical reagents were purchased from Thermo Fisher (Pittsburgh, PA), unless otherwise specified. Media for culturing *Cryptococcus* were either Sabouraud dextrose agar, or yeast extract-peptone-dextrose (YPD), containing Difco yeast extract, Bacto peptone, dextrose with and without 2% agar. Bovine serum albumin was added to 1X phosphate buffered saline (PBS) at a concentration of 0.5% as FACS buffer for flow cytometry staining. Complete medium for mouse cell culture was RPMI 1640 supplemented with 10% fetal bovine serum (FBS), 1% HEPES, 1% GlutaMAX and 1% Penicillin-Streptomycin. Where indicated, 0.5 µg/ml amphotericin B was included in the complete medium.

Mouse Strains

Experiments were performed using 6-10 weeks old male and female mice in approximately equal numbers. BALB/c and C57BL/6 WT mice were obtained from The Jackson Laboratory (Bar Harbor, ME). B cell deficient $Jh^{-/-}$ mice on the BALB/c background were purchased from Taconic Biosciences (Rensselaer, NY). B cell deficient (µMT, JAX stock #002288), CD4-

deficient (MHCII$^{-/-}$, JAX stock #003239), and CD8-deficient (β2m$^{-/-}$, JAX stock #002087) mice on the C57BL/6 background were obtained from The Jackson Laboratory. Knockout mice on the C57BL/6 background deficient in IFNɣ (IFNɣ$^{-/-}$, JAX stock #002287), IFNɣR (IFNɣR$^{-/-}$, JAX stock #003288), TNFα (TNFα$^{-/-}$, JAX stock #005540), IL-1β (IL-1β$^{-/-}$, JAX stock #68082), IL-6 (IL-6$^{-/-}$, JAX stock #002650), and IL-23p19 (IL-23$^{-/-}$) were also obtained from The Jackson Laboratory, except for the IL-23$^{-/-}$ mice which were from Nico Ghilardi (Genentech, South San Francisco, CA)[57]. Mice were bred and housed in specific pathogen-free conditions in the animal facilities at the University of Massachusetts Chan Medical School (UMCMS). All animal care and procedures were in accordance with protocols approved by the UMCMS Institutional Animal Care and Use Committee.

Cryptococcus neoformans

C. neoformans var. grubii strain KN99α[58], hereafter referred to as KN99, was preserved in 50% glycerol at -80°C. To prepare fungal cells for infection, KN99 was grown on YPD agar for 48h at 30°C, followed by overnight culture in 4mL liquid YPD at 30°C with shaking. Cells were washed three times with 1X PBS buffer, and the concentration of yeast cells was determined using an T20 automated cell counter (BioRad, Hercules, CA). CFUs were quantified by culturing on Sabouraud dextrose agar.

To prepare heat-killed (HK) *C. neoformans* as stimuli for *ex vivo* experiments, KN99 was shaken 18h in YPD liquid medium at 30°C, then diluted 1:200 into fresh YPD medium and shaken for 48h. The number of cells was determined and the culture was diluted with PBS to 2.6 x10^{7} cells/ml which is equivalent in dry weight to 1 mg/ml. The fungi were heat-killed at 70°C for 30min, and then aliquoted without further washing and stored at -80°C until use. Complete fungal killing was confirmed by the absence of CFU following plating on Sabouraud dextrose agar.

GP-Vaccines

Cryptococcal proteins Cda1 and Cda2 were expressed in *E. coli* and purified as described[16]. Briefly, the cDNAs encoding for Cda1 and Cda2 protein were synthesized and cloned in the pET-19b vector by GenScript (Piscataway NJ). Recombinant proteins were purified on HisBind resin (MilliporeSigma, Burlington, MA) and dialyzed against 6M urea/20mM Tris-HCl, pH 7.9. Protein concentrations were determined using the bicinchoninic acid (BCA) assay. Protein purity was assessed by SDS-PAGE (BioRad) followed by staining with InstantBlue Coomassie Protein Stain (Abcam, Cambridge, UK). Proteins were concentrated using Amicon Ultra-15 centrifugal filters (10K MWCO; MilliporeSigma) and adjusted to a concentration of 10 mg/ml. GP-Cda1 and GP-Cda2 vaccines were prepared as described[47]. Each vaccine dose consisted of a 100 µl sterile 0.9% saline suspension of 200 µg GPs (approximately 10^8 GP particles) containing 10 µg of recombinant protein and 25 µg of mouse serum albumin (MSA) complexed with yeast RNA (yRNA).

Immunization and Infection Strategy

Vaccines were administered to mice subcutaneously near the midline of abdomen as a prime dose followed by two boosters, with a 2-week interval between each injection. The GP-Cda1/Cda2 two antigen combination vaccine followed the same schedule and was formulated such that a single 100 µl dose consisted of a 1:1 mix of GP-Cda1 and GP-Cda2 containing 5 µg of each protein. Two weeks after the last vaccination, mice were anesthetized with 2% isoflurane (Covetrus, Portland, ME) inhalation and orotracheally inoculated with *C. neoformans* suspended in 50 µl PBS. The inoculum was 2 x 10^4 yeast cells for WT and knockout mice on the BALB/c background, and 1 x 10^4 cells for WT and knockout mice on the C57BL/6 background. For the survival studies, mice were monitored daily until 70 dpi at which point the experiment was terminated and remaining mice were euthanized with CO_2 asphyxiation. For the *ex vivo* immunology experiments, mice were euthanized at the indicated time points.

CD4+ T cell Depletion

The anti-CD4 monoclonal antibody GK1.5 (Cell Culture Company, Minneapolis, MN) was used to deplete $CD4^+$ T cells. Mice received the indicated dose of GK1.5 intraperitoneally in 100 µl PBS. Control mice received 100 µl intraperitoneal PBS. $CD4^+$ T cell counts in peripheral blood were assessed by performing cheek bleeds in uninfected BALB/c mice. Four mice per dosage group were studied, so that two mice per group were assessed each week and two weeks elapsed between blood collections from the same mice. For each sample, 100 µl whole blood was obtained and divided into technical duplicates for staining with CD3-PE, CD4-PerCP-Cyanine5.5 and CD8-APC antibodies (BioLegend, San Diego, CA), followed by red blood cell lysis and fixation with 1 ml 1X RBC Lysis/Fixation Solution (BioLegend). Cells were then centrifuged at 350 x g for 5 min after which the pellets were resuspended with 275 µl FACS buffer and 25 µl of CountBright Absolute Counting Beads. Cells were analyzed on a 5-laser Bio-Rad ZE5 flow cytometer.

Single Cell Suspension Preparation and Lung CFU Detection

Following anesthesia with isoflurane, blood was drawn by cardiac puncture with heparinized syringes and pooled within experimental groups. The blood was diluted with an equal volume of PBS containing 2% FBS, then layered over 5 ml of Ficoll-Paque PREMIUM 1.084 (Cytiva, Uppsala, Sweden) in 15 ml SepMate-50 tubes (STEM Cell Technology, Cambridge, MA). After centrifugation at 1200 x g for 20 min, the interphase containing PBMCs was collected. Spleens and lungs were dissociated after cardiac puncture and analyzed individually. Spleens were pressed with the piston of a 3 ml syringe and through a 70 µm cell strainer with 6 ml complete media to collect single cells. Lung single-cell suspensions were prepared using the MACS Lung Dissociation Kit for mouse as described by the manufacturer (Miltenyi Biotec, Bergisch Gladbach, Germany). Single-cell suspensions of the lungs were enriched for leukocytes using a 67% and 40% Percoll (Cytiva) gradient, followed by collection of interphase cells. Single cells

from the blood, spleen and lungs were washed and resuspended in complete culture medium supplemented with amphotericin B. The concentration and viability of cells were determined with Trypan blue (BioRad) using a T20 auto cell counter. For lungs collected at 10 dpi or 70 dpi, undiluted and diluted lung single cell suspensions were plated on Sabouraud dextrose agar, and incubated at 30°C for 2-3 days, at which time CFUs of *Cryptococcus* were counted. The detection limit was 20 CFU/lung.

Ex Vivo **Cell Culture and Stimulation**

PBMCs, splenocytes, and lung leukocytes were plated in tissue culture-treated 96-well round bottom plates at 2 x 10^5, 1 x 10^6, and 4 x 10^5 cells/well, respectively. Cells were left unstimulated or stimulated with Cda1 or Cda2 protein (5 µg/ml), HK *C. neoformans* strain KN99 (50 µg/ml), or Staphylococcal Enterotoxin B (SEB, 1 µg/ml; Toxin Technology Inc, Sarasota, FL). Incubations were performed at 37°C in humidified air supplemented with 5% CO_2. PBMCs and splenocytes were cultured 3 days following which supernatants were collected and stored at -80°C pending assay for IFNɣ. For lung leukocytes, cells were cultured for 18h. Brefeldin A (5 µg/ml, BioLegend) was added for the last 4h of lung leukocytes and PBMCs culture. Duplicates or triplicates were conducted for each sample. Culture supernatants were collected and stored at -80°C for subsequent IFNɣ measurements, while the lung leukocytes were analyzed by flow cytometry.

Quantification of IFNɣ Production

IFNɣ concentrations in cell supernatants were determined with the R&D Systems Mouse IFNɣ DuoSet ELISA Kit (Bio-Techne, Minneapolis, MN) according to the manufacturer's protocol. Samples were run in 1:2 dilutions. The detection limit was 10 pg/ml. Values lower than the detection limit were arbitrarily assigned a value of 9 pg/ml.

Intracellular Staining and FACS Analysis

Lung leukocytes were stained with LIVE/DEAD green fixable dead cell stain kit. Cell surface antigens were then stained with CD3-PE, CD4-PerCP/Cyanine5.5, and CD8-APC (BioLegend). After fixation and permeabilization using the Intracellular Fixation & Permeabilization Buffer Set, cells were co-incubated with rat anti-mouse CD16/CD32 monoclonal antibody 2.4G2 (BD Pharmingen) to block Fc receptors, and then stained with CD154-PE/Cyanine7, IFNɣ-BV650, IL17A-BV510, and TNFα-APC/Cyanine7 (BioLegend). FACS data were acquired with a 5-laser BD LSRII flow cytometer and analyzed using FlowJo version 10.8 software (BD, Franklin Lakes, NJ). Gating was established using FMO controls and isotype controls. Briefly, a singlet gate was created on a plot of forward scatter height (FSC-H) vs. FSC-A. Then, debris were excluded based on FSC-A and side scatter area (SSC-A). The dead cells were excluded using the LIVE/DEAD green signal, the $CD4^+CD8^-$ population was selected from the $CD3^+$ population, and finally the expression of IFNγ, IL-17A, TNFα and CD154 by the live $CD3^+CD4^+CD8^-$ gated population was examined (see supplemental Fig. 1S). An identical gating strategy was used to examine $CD8^+$ T cells except the $CD4^-CD8^+$ population was selected from the $CD3^+$ population.

Statistics

Data were analyzed and graphs were drawn using GraphPad Prism, version 9.2.0 (GraphPad Software, La Jolla, CA). Kaplan-Meier survival curves were analyzed for significance using the Mantel Cox log rank test. When median survival differences were ≤3d, findings were not considered biologically significant and thus not denoted as statistically significant. Lung CFUs were compared using the Mann-Whitney test. Lung leukocytes, $CD4^+$ T cell and $CD8^+$ T cell numbers in groups were compared using the one-way ANOVA test with Bonferroni's correction for multiple comparison. For the *ex vivo* experiments, technical triplicates of pooled PBMC in each group were presented and analyzed. Averages of technical duplicates or triplicates for each sample were presented and data were analyzed individually for spleen and lungs. The comparisons of cytokine expression among groups were performed by two-way ANOVA test

with Bonferroni's correction applied for multiple comparisons. Significance was defined as a *P* value of <0.05 following corrections for multiple comparisons.

Reporting summary

Further information on research design is available in the Nature Research Reporting Summary linked to this article.

DATA AVAILABILITY

The datasets generated during and/or analyzed during the current study are available from the corresponding author on reasonable request.

AUTHOR CONTRIBUTIONS

R.W., L.V.N.O., M.M.H., S.M.L, C.A.S, and G.R.O. conceived and designed experiments. R.W., L.V.N.O., D.L., C.L.G., C.K.L., Z.M, M.M.H., and C.A.S performed experiments. R.W., L.V.N.O., C.A.S., and S.M.L. analyzed the data. R.W., L.V.N.O., C.A.S., and S.M.L. wrote the paper. All authors contributed to the manuscript and approved the submitted version.

COMPETING INTEREST STATEMENT

The authors declare that the research was conducted in the absence of any commercial or financial relationships that could be construed as a potential conflict of interest.

ACKNOWLEDGMENTS

This research was supported by National Institute of Allergy and Infectious Diseases, National Institutes of Health grants R01 AI172154, R01 AI025780, R01 AI102618, R01 AI125045, R01 AI139615, and R01 AI072195, and contract 75N93019C00064. M.M.H. was partially supported by NIH Training Grant T32 AI095213. The authors thank Ambily Abraham for her assistance in preparing the GP vaccines.

REFERENCES

1 May, R. C., Stone, N. R., Wiesner, D. L., Bicanic, T. & Nielsen, K. Cryptococcus: from environmental saprophyte to global pathogen. *Nat Rev Microbiol* **14**, 106-117, doi:10.1038/nrmicro.2015.6 (2016).

2 Stott, K. E. *et al.* Cryptococcal meningoencephalitis: time for action. *Lancet Infect Dis* **21**, e259-e271, doi:10.1016/S1473-3099(20)30771-4 (2021).

3 Rajasingham, R. *et al.* The global burden of HIV-associated cryptococcal infection in adults in 2020: a modelling analysis. *Lancet Infect Dis*, doi:10.1016/S1473-3099(22)00499-6 (2022).

4 Iyer, K. R., Revie, N. M., Fu, C., Robbins, N. & Cowen, L. E. Treatment strategies for cryptococcal infection: challenges, advances and future outlook. *Nat Rev Microbiol* **19**, 454-466, doi:10.1038/s41579-021-00511-0 (2021).

5 Oliveira, L. V. N., Wang, R., Specht, C. A. & Levitz, S. M. Vaccines for human fungal diseases: close but still a long way to go. *NPJ Vaccines* **6**, 33, doi:10.1038/s41541-021-00294-8 (2021).

6 Wang, Y., Wang, K., Masso-Silva, J. A., Rivera, A. & Xue, C. A Heat-Killed Cryptococcus Mutant Strain Induces Host Protection against Multiple Invasive Mycoses in a Murine Vaccine Model. *mBio* **10**, 02145, doi:10.1128/mBio.02145-19 (2019).

7 Colombo, A. C. *et al.* Cryptococcus neoformans Glucuronoxylomannan and Sterylglucoside Are Required for Host Protection in an Animal Vaccination Model. *mBio* **10**, e02909-02918, doi:10.1128/mBio.02909-18 (2019).

8 Upadhya, R. *et al.* Induction of Protective Immunity to Cryptococcal Infection in Mice by a Heat-Killed, Chitosan-Deficient Strain of Cryptococcus neoformans. *mBio* **7**, e00547-00516, doi:10.1128/mBio.00547-16 (2016).

9 Ueno, K., Yanagihara, N., Shimizu, K. & Miyazaki, Y. Vaccines and Protective Immune Memory against Cryptococcosis. *Biol Pharm Bull* **43**, 230-239, doi:10.1248/bpb.b19-00841 (2020).

10 Zhai, B. *et al.* Development of Protective Inflammation and Cell-Mediated Immunity against Cryptococcus neoformans after Exposure to Hyphal Mutants. *mBio* **6**, e01433-01415, doi:10.1128/mBio.01433-15 (2015).

11 Wormley, F. L., Jr., Perfect, J. R., Steele, C. & Cox, G. M. Protection against cryptococcosis by using a murine gamma interferon-producing Cryptococcus neoformans strain. *Infection and immunity* **75**, 1453-1462, doi:10.1128/IAI.00274-06 (2007).

12 Van Dyke, M. C. C. *et al.* Induction of Broad-Spectrum Protective Immunity against Disparate Cryptococcus Serotypes. *Frontiers in Immunology* **8**, 1-16, doi:10.3389/fimmu.2017.01359 (2017).

13 Upadhya, R. *et al.* Cryptococcus neoformans Cda1 and Cda2 coordinate deacetylation of chitin during infection to control fungal virulence. *Cell Surf* **7**, 100066, doi:10.1016/j.tcsw.2021.100066 (2021).

14 Specht, C. A. *et al.* Vaccination with Recombinant Cryptococcus Proteins in Glucan Particles Protects Mice against Cryptococcosis in a Manner Dependent upon Mouse Strain and Cryptococcal Species. *MBio* **8**, doi:10.1128/mBio.01872-17 (2017).

15 Specht, C. A. *et al.* Protection of Mice against Experimental Cryptococcosis by Synthesized Peptides Delivered in Glucan Particles. *mBio*, e0336721, doi:10.1128/mbio.03367-21 (2022).

16 Hester, M. M. *et al.* Protection of mice against experimental cryptococcosis using glucan particle-based vaccines containing novel recombinant antigens. *Vaccine* **38**, 620-626, doi:10.1016/j.vaccine.2019.10.051 (2020).

17 Kitamura, D., Roes, J., Kuhn, R. & Rajewsky, K. A B cell-deficient mouse by targeted disruption of the membrane exon of the immunoglobulin mu chain gene. *Nature* **350**, 423-426, doi:10.1038/350423a0 (1991).
18 Chen, J. *et al.* Immunoglobulin gene rearrangement in B cell deficient mice generated by targeted deletion of the JH locus. *Int Immunol* **5**, 647-656, doi:10.1093/intimm/5.6.647 (1993).
19 Lionakis, M. S. & Levitz, S. M. Host Control of Fungal Infections: Lessons from Basic Studies and Human Cohorts. *Annu Rev Immunol* **36**, 157-191, doi:10.1146/annurev-immunol-042617-053318 (2018).
20 Lee, J. S. *et al.* Observed CD4 counts at entry into HIV care and at antiretroviral therapy prescription by age in the USA, 2004-18: a cohort study. *Lancet HIV* **9 Suppl 1**, S2, doi:10.1016/S2352-3018(22)00067-4 (2022).
21 Mukaremera, L. & Nielsen, K. Adaptive Immunity to Cryptococcus neoformans Infections. *J Fungi (Basel)* **3**, doi:10.3390/jof3040064 (2017).
22 Jarvis, J. N. *et al.* Adjunctive interferon-gamma immunotherapy for the treatment of HIV-associated cryptococcal meningitis: a randomized controlled trial. *AIDS* **26**, 1105-1113, doi:10.1097/QAD.0b013e3283536a93 (2012).
23 Williamson, P. R. *et al.* Cryptococcal meningitis: epidemiology, immunology, diagnosis and therapy. *Nat Rev Neurol* **13**, 13-24, doi:10.1038/nrneurol.2016.167 (2017).
24 George, I. A., Spec, A., Powderly, W. G. & Santos, C. A. Q. Comparative Epidemiology and Outcomes of Human Immunodeficiency virus (HIV), Non-HIV Non-transplant, and Solid Organ Transplant Associated Cryptococcosis: A Population-Based Study. *Clin Infect Dis* **66**, 608-611, doi:10.1093/cid/cix867 (2018).
25 Subramaniam, K. *et al.* IgM(+) memory B cell expression predicts HIV-associated cryptococcosis status. *J Infect Dis* **200**, 244-251, doi:10.1086/599318 (2009).
26 Lindell, D. M., Moore, T. A., McDonald, R. A., Toews, G. B. & Huffnagle, G. B. Generation of antifungal effector CD8+ T cells in the absence of CD4+ T cells during Cryptococcus neoformans infection. *J Immunol* **174**, 7920-7928, doi:10.4049/jimmunol.174.12.7920 (2005).
27 Rohatgi, S. *et al.* Fc gamma receptor 3A polymorphism and risk for HIV-associated cryptococcal disease. *mBio* **4**, e00573-00513, doi:10.1128/mBio.00573-13 (2013).
28 Szymczak, W. A. *et al.* X-linked immunodeficient mice exhibit enhanced susceptibility to Cryptococcus neoformans Infection. *mBio* **4**, doi:10.1128/mBio.00265-13 (2013).
29 Mukherjee, J., Scharff, M. D. & Casadevall, A. Protective murine monoclonal antibodies to Cryptococcus neoformans. *Infect Immun* **60**, 4534-4541, doi:10.1128/iai.60.11.4534-4541.1992 (1992).
30 Devi, S. J. Preclinical efficacy of a glucuronoxylomannan-tetanus toxoid conjugate vaccine of Cryptococcus neoformans in a murine model. *Vaccine* **14**, 841-844 (1996).
31 Datta, K., Lees, A. & Pirofski, L. A. Therapeutic efficacy of a conjugate vaccine containing a peptide mimotope of cryptococcal capsular polysaccharide glucuronoxylomannan. *Clin Vaccine Immunol* **15**, 1176-1187, doi:10.1128/CVI.00130-08 (2008).
32 Aguirre, K. M. & Johnson, L. L. A role for B cells in resistance to Cryptococcus neoformans in mice. *Infect Immun* **65**, 525-530, doi:10.1128/iai.65.2.525-530.1997 (1997).
33 Wozniak, K. L. *et al.* Insights into the mechanisms of protective immunity against Cryptococcus neoformans infection using a mouse model of pulmonary cryptococcosis. *PLoS One* **4**, e6854, doi:10.1371/journal.pone.0006854 (2009).
34 Hill, J. O. & Harmsen, A. G. Intrapulmonary growth and dissemination of an avirulent strain of Cryptococcus neoformans in mice depleted of CD4+ or CD8+ T cells. *J Exp Med* **173**, 755-758, doi:10.1084/jem.173.3.755 (1991).

35 Huffnagle, G. B., Yates, J. L. & Lipscomb, M. F. Immunity to a pulmonary Cryptococcus neoformans infection requires both CD4+ and CD8+ T cells. *J Exp Med* **173**, 793-800, doi:10.1084/jem.173.4.793 (1991).
36 Huffnagle, G. B., Lipscomb, M. F., Lovchik, J. A., Hoag, K. A. & Street, N. E. The role of CD4+ and CD8+ T cells in the protective inflammatory response to a pulmonary cryptococcal infection. *J Leukoc Biol* **55**, 35-42, doi:10.1002/jlb.55.1.35 (1994).
37 Nanjappa, S. G., Heninger, E., Wuthrich, M., Gasper, D. J. & Klein, B. S. Tc17 cells mediate vaccine immunity against lethal fungal pneumonia in immune deficient hosts lacking CD4+ T cells. *PLoS Pathog* **8**, e1002771, doi:10.1371/journal.ppat.1002771 (2012).
38 Fernandez-Ruiz, M. *et al.* Kinetics of peripheral blood lymphocyte subpopulations predicts the occurrence of opportunistic infection after kidney transplantation. *Transpl Int* **27**, 674-685, doi:10.1111/tri.12321 (2014).
39 Jarvis, J. N. *et al.* Single-Dose Liposomal Amphotericin B Treatment for Cryptococcal Meningitis. *N Engl J Med* **386**, 1109-1120, doi:10.1056/NEJMoa2111904 (2022).
40 Garcia-Hermoso, D., Janbon, G. & Dromer, F. Epidemiological evidence for dormant Cryptococcus neoformans infection. *J Clin Microbiol* **37**, 3204-3209, doi:10.1128/JCM.37.10.3204-3209.1999 (1999).
41 Brunet, K., Alanio, A., Lortholary, O. & Rammaert, B. Reactivation of dormant/latent fungal infection. *J Infect* **77**, 463-468, doi:10.1016/j.jinf.2018.06.016 (2018).
42 Cassone, A. Fungal vaccines: real progress from real challenges. *Lancet Infect Dis* **8**, 114-124, doi:10.1016/S1473-3099(08)70016-1 (2008).
43 Portuondo, D. L., Ferreira, L. S., Urbaczek, A. C., Batista-Duharte, A. & Carlos, I. Z. Adjuvants and delivery systems for antifungal vaccines: current state and future developments. *Med Mycol* **53**, 69-89, doi:10.1093/mmy/myu045 (2015).
44 Elsegeiny, W., Marr, K. A. & Williamson, P. R. Immunology of Cryptococcal Infections: Developing a Rational Approach to Patient Therapy. *Front Immunol* **9**, 651, doi:10.3389/fimmu.2018.00651 (2018).
45 Scriven, J. E. *et al.* Early ART After Cryptococcal Meningitis Is Associated With Cerebrospinal Fluid Pleocytosis and Macrophage Activation in a Multisite Randomized Trial. *J Infect Dis* **212**, 769-778, doi:10.1093/infdis/jiv067 (2015).
46 Zhang, Y. *et al.* Robust Th1 and Th17 immunity supports pulmonary clearance but cannot prevent systemic dissemination of highly virulent Cryptococcus neoformans H99. *Am J Pathol* **175**, 2489-2500, doi:10.2353/ajpath.2009.090530 (2009).
47 Huang, H., Ostroff, G. R., Lee, C. K., Specht, C. A. & Levitz, S. M. Robust stimulation of humoral and cellular immune responses following vaccination with antigen-loaded beta-glucan particles. *mBio* **1**, doi:10.1128/mBio.00164-10 (2010).
48 Abraham, A., Ostroff, G., Levitz, S. M. & Oyston, P. C. F. A novel vaccine platform using glucan particles for induction of protective responses against Francisella tularensis and other pathogens. *Clin Exp Immunol* **198**, 143-152, doi:10.1111/cei.13356 (2019).
49 Deepe, G. S., Jr. *et al.* Vaccination with an alkaline extract of Histoplasma capsulatum packaged in glucan particles confers protective immunity in mice. *Vaccine* **36**, 3359-3367, doi:10.1016/j.vaccine.2018.04.047 (2018).
50 Kak, G., Raza, M. & Tiwari, B. K. Interferon-gamma (IFN-gamma): Exploring its implications in infectious diseases. *Biomol Concepts* **9**, 64-79, doi:10.1515/bmc-2018-0007 (2018).
51 Kleinschek, M. A. *et al.* IL-23 enhances the inflammatory cell response in Cryptococcus neoformans infection and induces a cytokine pattern distinct from IL-12. *J Immunol* **176**, 1098-1106 (2006).

52 Tanaka, T., Narazaki, M. & Kishimoto, T. IL-6 in inflammation, immunity, and disease. *Cold Spring Harb Perspect Biol* **6**, a016295, doi:10.1101/cshperspect.a016295 (2014).
53 Gaffen, S. L., Jain, R., Garg, A. V. & Cua, D. J. The IL-23-IL-17 immune axis: from mechanisms to therapeutic testing. *Nat Rev Immunol* **14**, 585-600, doi:10.1038/nri3707 (2014).
54 Beenhouwer, D. O., Shapiro, S., Feldmesser, M., Casadevall, A. & Scharff, M. D. Both Th1 and Th2 cytokines affect the ability of monoclonal antibodies to protect mice against Cryptococcus neoformans. *Infect Immun* **69**, 6445-6455, doi:10.1128/IAI.69.10.6445-6455.2001 (2001).
55 Levitz, S. M., Tabuni, A., Kornfeld, H., Reardon, C. C. & Golenbock, D. T. Production of tumor necrosis factor alpha in human leukocytes stimulated by Cryptococcus neoformans. *Infect Immun* **62**, 1975-1981, doi:10.1128/IAI.62.5.1975-1981.1994 (1994).
56 Chen, M. *et al.* Internalized Cryptococcus neoformans Activates the Canonical Caspase-1 and the Noncanonical Caspase-8 Inflammasomes. *J Immunol* **195**, 4962-4972, doi:10.4049/jimmunol.1500865 (2015).
57 Ghilardi, N. *et al.* Compromised humoral and delayed-type hypersensitivity responses in IL-23-deficient mice. *J Immunol* **172**, 2827-2833, doi:10.4049/jimmunol.172.5.2827 (2004).
58 Janbon, G. *et al.* Analysis of the genome and transcriptome of Cryptococcus neoformans var. grubii reveals complex RNA expression and microevolution leading to virulence attenuation. *PLoS Genet* **10**, e1004261, doi:10.1371/journal.pgen.1004261 (2014).

Figure Legends

Fig. 1. Contribution of B cells to protection by GP-Cda1 or GP-Cda2 vaccines. WT C57BL/6 mice and B cell-deficient (μMT) mice on the C57BL/6 background (A and B), and WT BALB/c mice and B cell-deficient (Jh-/-) mice (C and D) on the BALB/c background received a prime and two biweekly boosts with the indicated GP-Cda1 or GP-Cda2 vaccine. Two weeks after the last boost, mice were challenged with C. neoformans and then followed 70d for survival. Vac = vaccinated with GP-Cda1 or GP-Cda2. UnVac = unvaccinated. n denotes the number of mice in the experimental group. Note the same survival curves are shown for unvaccinated mice in Fig. 1A and 1B as well as in Fig. 1C and 1D. Within each group of WT and mutant mouse strains, $P < 0.0005$ comparing Vac and UnVac mice (A, B, C and D).

Fig. 2. Contribution of CD8+ and CD4+ T cells to protection by GP-Cda1 or GP-Cda2. Top panel: Wild-type (WT) C57BL/6 mice and CD8+ T cell-deficient (β2m) mice on the C57BL/6 background received a prime and two biweekly boosts with GP-Cda1 (A) or GP-Cda2 (B). Two weeks after the last boost, mice were challenged with C. neoformans and followed 70 days for survival. Vac = vaccinated with GP-Cda1 or GP-Cda2. UnVac = unvaccinated. n denotes the number of mice in the experimental group. Bottom panel: Same as the top panel except CD4+ T cell-deficient (MHCII-/-) mice were used (C and D). Note the same survival curves are shown for unvaccinated mice in Fig. 2A and 2B as well as in Fig. 2C and 2D. $P < 0.005$ when comparing WT Vac vs WT UnVac (A, B, C and D), mutant Vac vs mutant UnVac (A, B and D), and WT Vac vs mutant Vac (C and D).

Fig. 3. Effect of CD4+ T cell depletion during the vaccination and challenge phases on GP-Cda2 protection. (A) Experimental outline. BALB/c mice received a prime and two biweekly

boosts of the GP-Cda2 vaccine (Vac) followed by a pulmonary challenge with C. neoformans. The CD4-depleting mAb GK1.5 was administered at three biweekly intervals either during the vaccination phase (Vac Phase) 2d before each vaccine dose or the challenge phase (Chal Phase) with the first dose given 2d before C. neoformans challenge. Controls included vaccinated mice that did not get GK1.5 (No GK1.5) and unvaccinated (UnVac) mice. (B) Kaplan-Meier survival curve of mice followed for 70 days (10 weeks) after challenge, with percent survival recorded daily. Data are from two independent experiments, each with 5 mice/group. Significant ($P<0.001$, Mantel-Cox log rank test) survival compared with unvaccinated mice was seen only for mice that did not get GK1.5.

Fig. 4. The effect of partial CD4+ T cell depletion on vaccine-mediated protection. (A) Naïve BALB/c mice were injected with the indicated amount of anti-CD4 mAb GK1.5 on day -2. Every other week starting on day 0, the mice underwent cheek bleeds to determine the CD4+ T cell count in peripheral blood. Four mice per group were studied, staggered so that two mice per group were tested each week. Data are mean values. (B) BALB/c mice were vaccinated thrice at biweekly intervals with GP-Cda1/Cda2. Twelve days after the last boost, mice were injected with the indicated amount of GK1.5. Two days later, the mice received a pulmonary challenge with C. neoformans and monitored for survival until day 70. UnVac = Unvaccinated. Data are from two independent experiments, each with 5 mice/group. Significant ($P<0.005$) survival compared with unvaccinated mice was seen for those groups of mice receiving a GK1.5 dose $\leqslant$ 40 µg.

Fig. 5. IFNɣ production by ex vivo stimulated PBMCs, splenocytes, and lung leukocytes following GP-Cda1/Cda2 vaccination and/or infection. BALB/c mice were vaccinated thrice

at biweekly intervals with GP-Cda1/Cda2. Two weeks after last boost, the mice received a pulmonary challenge with C. neoformans. Mice were euthanized at 0 dpi (uninfected), 10 dpi or 70 dpi. PBMCs (A), spleens (B), and lungs (C) were collected. Controls included unvaccinated mice that were euthanized at 0 dpi or 10 dpi. Single cell PBMC, spleen, and lung suspensions were prepared following which cells were cultured in complete media supplemented with amphotericin B in the presence of the indicated antigens for either 3 days (PBMC and spleen) or 18h (lung). Control cells were left unstimulated (Unstim). Supernatants were collected and analyzed for IFNɣ by ELISA. Each group had 5 mice. Vac, vaccinated with GP-Cda1/Cda2. Chall, challenged with C. neoformans strain KN99. Dpi, days post infection, HK KN99, heat-killed C. neoformans strain KN99. IFNɣ production following SEB stimulation, as a positive control, was shown in Fig. 2S. The results of the statistical comparisons between groups were shown in Fig. 3S.

Fig. 6. Analysis of lung CFU, leukocytes, and ex vivo antigen-stimulated Th intracellular cytokine production following GP-Cda1/Cda2 vaccination and/or infection. BALB/c mice were vaccinated thrice at biweekly intervals with GP-Cda1/Cda2. Two weeks after last boost, the mice received a pulmonary challenge with C. neoformans. Mice were euthanized at 0 dpi (uninfected), 10 dpi or 70 dpi. Controls included unvaccinated mice euthanized at 0 dpi or 10 dpi. Lungs were harvested and single cell suspensions were prepared. (A) CFU/lung were determined. (B) Leukocytes at the interface of a 67% and 40% Percoll gradient were collected and counted. (C-H) Leukocytes were cultured in complete media supplemented with amphotericin B and stimulated with indicated antigens or left unstimulated (Unstim) for 18h. Then the cells were collected, stained, and analyzed by polychromatic FACS, as described in Methods. (C, D) The numbers of CD4+ T and CD8+ T cells were calculated by multiplying the percentage of each population times the total leukocyte count. (E-H) The numbers of CD4+ T

cells expressing the activation marker CD154, or producing the intracellular cytokines IFNγ, IL-17, and TNFα following ex vivo stimulation. Each group had 5 mice. Vac = vaccinated with GP-Cda1/Cda2, Chall = challenge with C. neoformans, Dpi = days post infection, HK = heat killed. Statistical comparisons between groups are shown in Fig. 5S.

Fig. 7. Effect of host gene deletions in selected cytokines or cytokine receptor on GP-Cda1 or Cda2 vaccine efficacy. Wild-type (WT) mice and mice with selected cytokine or cytokine receptor deficiency (A. IFNɣ-/-; B. IFNɣR-/-; C. IL-6-/-; D. IL-23-/-; E. TNFα-/-; F. IL-1β-/-) received a prime and two biweekly boosts with GP-Cda1 or GP-Cda2. Two weeks after the last boost, mice were challenged with C. neoformans and followed 70 days for survival. UnVac = unvaccinated. n denotes the number of mice in the experimental group. All mice were on the C57BL/6 background. Note the same survival curves are shown for WT mice in Fig. 7A to 7F. For Fig. 7A-E, $P<0.001$ comparing survival between knockout and WT mice vaccinated with either GP-Cda1 or GP-Cda2. For Fig. 7F, $P<0.05$ comparing GP-Cda1-vaccinated IL-1β-/- and WT mice.

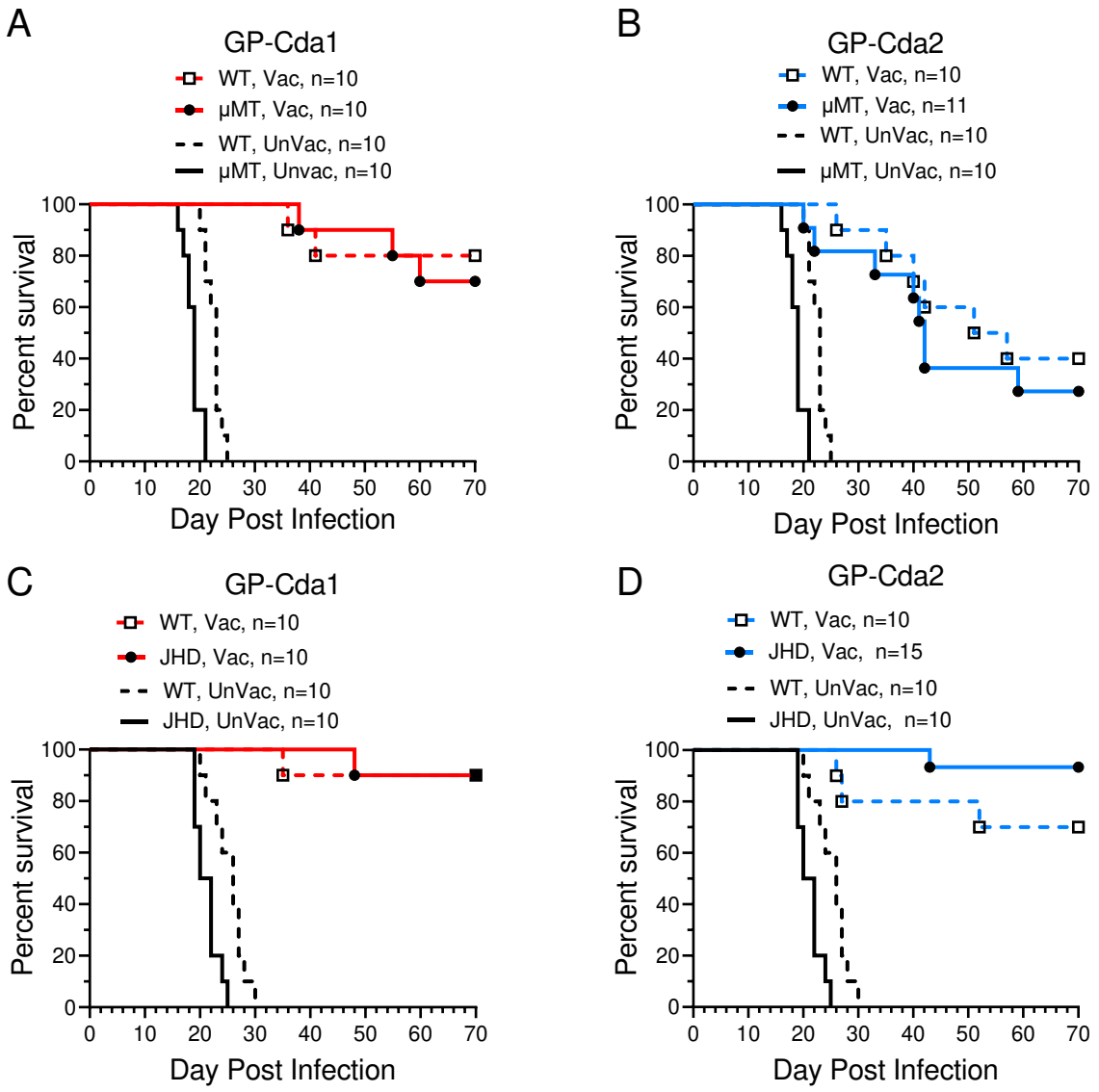

Fig. 1. Contribution of B cells to protection by GP-Cda1 or GP-Cda2 vaccines. WT C57BL/6 mice and B cell-deficient (µMT) mice on the C57BL/6 background (A and B), and WT BALB/c mice and B cell-deficient ($Jh^{-/-}$) mice (C and D) on the BALB/c background received a prime and two biweekly boosts with the indicated GP-Cda1 or GP-Cda2 vaccine. Two weeks after the last boost, mice were challenged with *C. neoformans* and then followed 70d for survival. Vac = vaccinated with GP-Cda1 or GP-Cda2. UnVac = unvaccinated. n denotes the number of mice in the experimental group. Note the same survival curves are shown for unvaccinated mice in Fig. 1A and 1B as well as in Fig. 1C and 1D. Within each group of WT and mutant mouse strains, $P < 0.0005$ comparing Vac and UnVac mice (A, B, C and D).

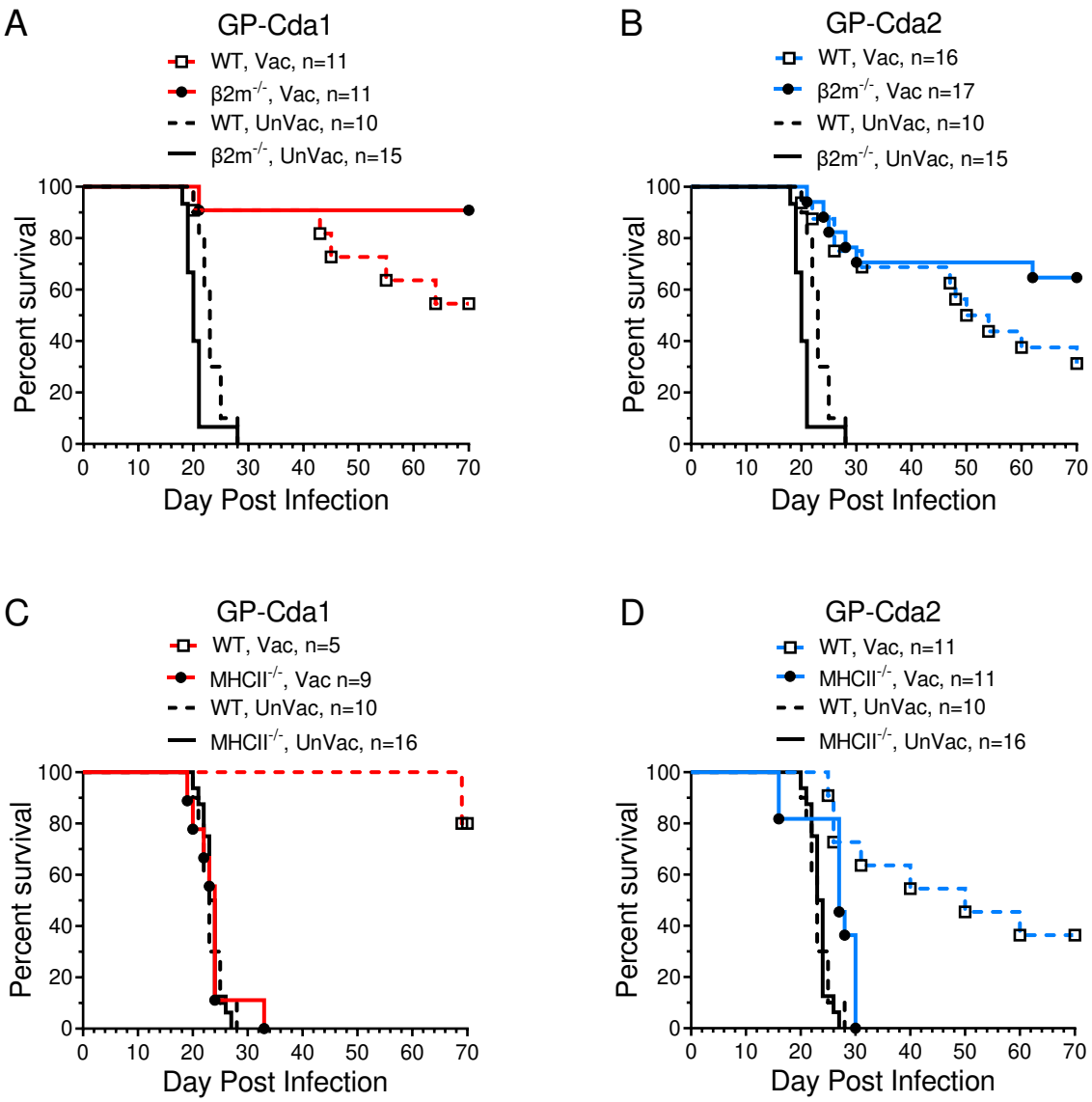

Fig. 2. **Contribution of CD8⁺ and CD4⁺ T cells to protection by GP-Cda1 or GP-Cda2.** Top panel: Wild-type (WT) C57BL/6 mice and CD8⁺ T cell-deficient (β2m) mice on the C57BL/6 background received a prime and two biweekly boosts with GP-Cda1 (A) or GP-Cda2 (B). Two weeks after the last boost, mice were challenged with *C. neoformans* and followed 70 days for survival. Vac = vaccinated with GP-Cda1 or GP-Cda2. UnVac = unvaccinated. n denotes the number of mice in the experimental group. Bottom panel: Same as the top panel except CD4⁺ T cell-deficient (MHCII$^{-/-}$) mice were used (C and D). Note the same survival curves are shown for unvaccinated mice in Fig. 2A and 2B as well as in Fig. 2C and 2D. $P < 0.005$ when comparing WT Vac vs WT UnVac (A, B, C and D), mutant Vac vs mutant UnVac (A, B and D), and WT Vac vs mutant Vac (C and D).

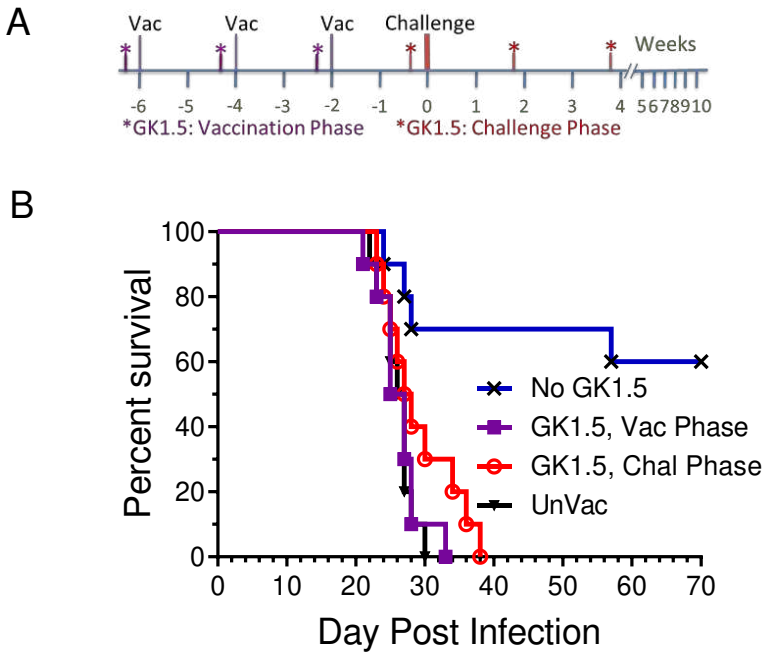

Fig. 3. Effect of CD4⁺ T cell depletion during the vaccination and challenge phases on GP-Cda2 protection. (A) Experimental outline. BALB/c mice received a prime and two biweekly boosts of the GP-Cda2 vaccine (Vac) followed by a pulmonary challenge with *C. neoformans*. The CD4-depleting mAb GK1.5 was administered at three biweekly intervals either during the vaccination phase (Vac Phase) 2d before each vaccine dose or the challenge phase (Chal Phase) with the first dose given 2d before *C. neoformans* challenge. Controls included vaccinated mice that did not get GK1.5 (No GK1.5) and unvaccinated (UnVac) mice. (B) Kaplan-Meier survival curve of mice followed for 70 days (10 weeks) after challenge, with percent survival recorded daily. Data are from two independent experiments, each with 5 mice/group. Significant (P<0.001, Mantel-Cox log rank test) survival compared with unvaccinated mice was seen only for mice that did not get GK1.5.

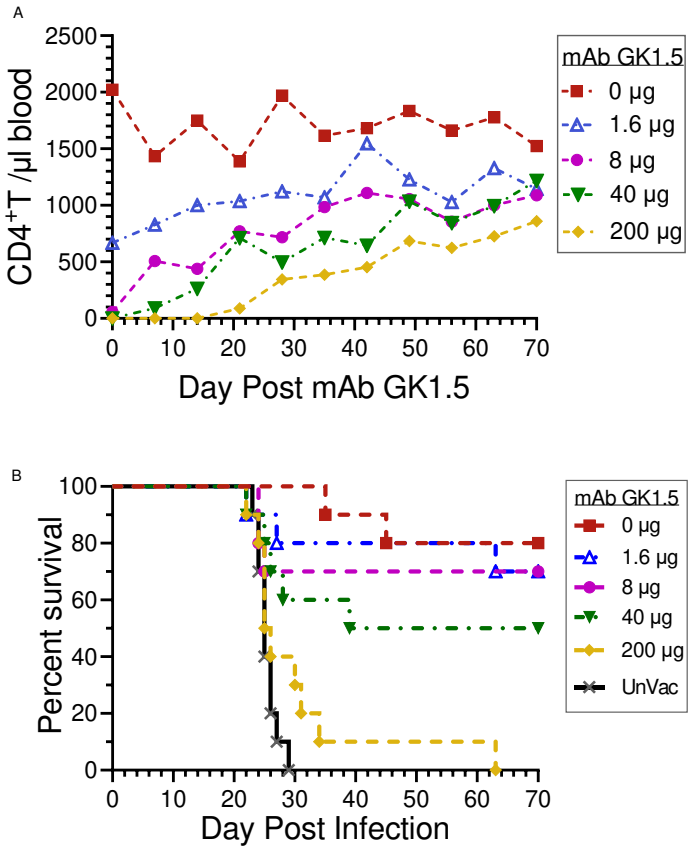

Fig. 4. The effect of partial CD4⁺ T cell depletion on vaccine-mediated protection. (A) Naïve BALB/c mice were injected with the indicated amount of anti-CD4 mAb GK1.5 on day -2. Every other week starting on day 0, the mice underwent cheek bleeds to determine the CD4⁺ T cell count in peripheral blood. Four mice per group were studied, staggered so that two mice per group were tested each week. Data are mean values. (B) BALB/c mice were vaccinated thrice at biweekly intervals with GP-Cda1/Cda2. Twelve days after the last boost, mice were injected with the indicated amount of GK1.5. Two days later, the mice received a pulmonary challenge with *C. neoformans* and monitored for survival until day 70. UnVac = Unvaccinated. Data are from two independent experiments, each with 5 mice/group. Significant (P<0.005) survival compared with unvaccinated mice was seen for those groups of mice receiving a GK1.5 dose ≤40 µg.

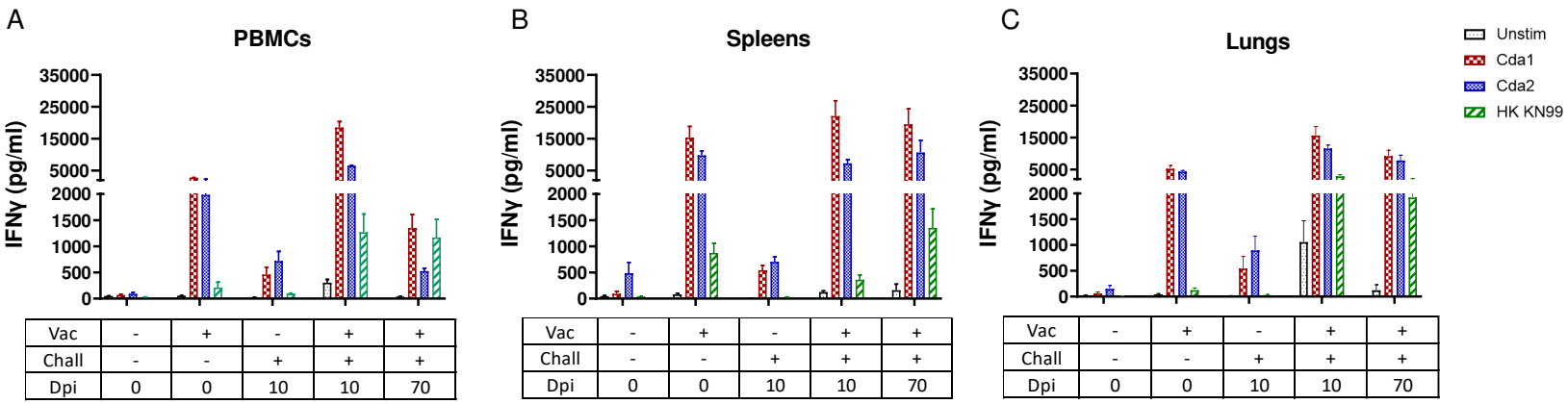

Fig. 5. IFNɣ production by *ex vivo* stimulated PBMCs, splenocytes, and lung leukocytes following GP-Cda1/Cda2 vaccination and/or infection. BALB/c mice were vaccinated thrice at biweekly intervals with GP-Cda1/Cda2. Two weeks after last boost, the mice received a pulmonary challenge with *C. neoformans*. Mice were euthanized at 0 dpi (uninfected), 10 dpi or 70 dpi. PBMCs (A), spleens (B), and lungs (C) were collected. Controls included unvaccinated mice that were euthanized at 0 dpi or 10 dpi. Single cell PBMC, spleen, and lung suspensions were prepared following which cells were cultured in complete media supplemented with amphotericin B in the presence of the indicated antigens for either 3 days (PBMC and spleen) or 18h (lung). Control cells were left unstimulated (Unstim). Supernatants were collected and analyzed for IFNɣ by ELISA. Each group had 5 mice. Vac, vaccinated with GP-Cda1/Cda2. Chall, challenged with *C. neoformans* strain KN99. Dpi, days post infection, HK KN99, heat-killed *C. neoformans* strain KN99. IFNɣ production following SEB stimulation, as a positive control, was shown in Fig. 2S. The results of the statistical comparisons between groups were shown in Fig. 3S.

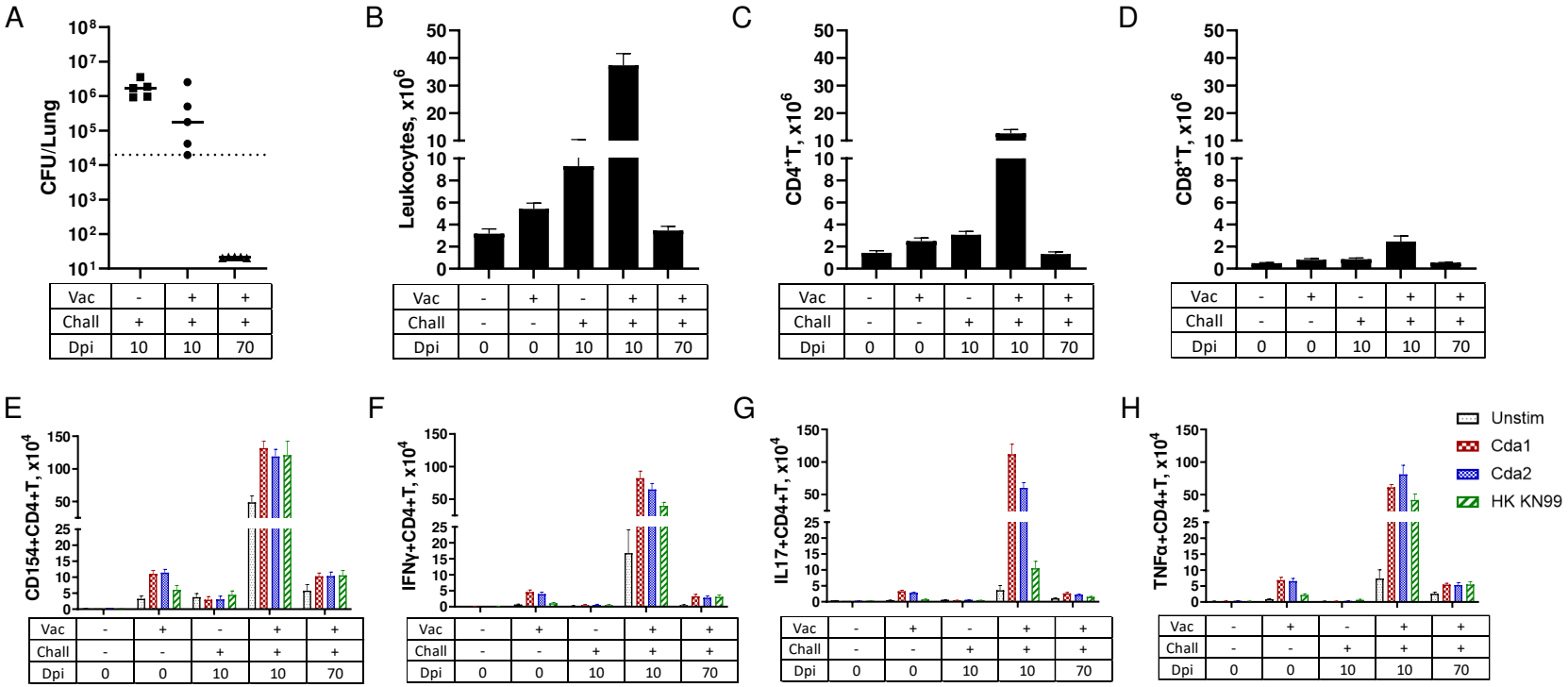

Fig. 6. Analysis of lung CFU, leukocytes, and *ex vivo* antigen-stimulated Th intracellular cytokine production following GP-Cda1/Cda2 vaccination and/or infection. BALB/c mice were vaccinated thrice at biweekly intervals with GP-Cda1/Cda2. Two weeks after last boost, the mice received a pulmonary challenge with *C. neoformans*. Mice were euthanized at 0 dpi (uninfected), 10 dpi or 70 dpi. Controls included unvaccinated mice euthanized at 0 dpi or 10 dpi. Lungs were harvested and single cell suspensions were prepared. (A) CFU/lung were determined. (B) Leukocytes at the interface of a 67% and 40% Percoll gradient were collected and counted. (C-H) Leukocytes were cultured in complete media supplemented with amphotericin B and stimulated with indicated antigens or left unstimulated (Unstim) for 18h. Then the cells were collected, stained, and analyzed by polychromatic FACS, as described in Methods. (C, D) The numbers of $CD4^+$ T and $CD8^+$ T cells were calculated by multiplying the percentage of each population times the total leukocyte count. (E-H) The numbers of $CD4^+$ T cells expressing the activation marker CD154, or producing the intracellular cytokines IFNγ, IL-17, and TNFα following *ex vivo* stimulation. Each group had 5 mice. Vac = vaccinated with GP-Cda1/Cda2, Chall = challenge with *C. neoformans*, Dpi = days post infection, HK = heat killed. Statistical comparisons between groups are shown in Fig. 5S.

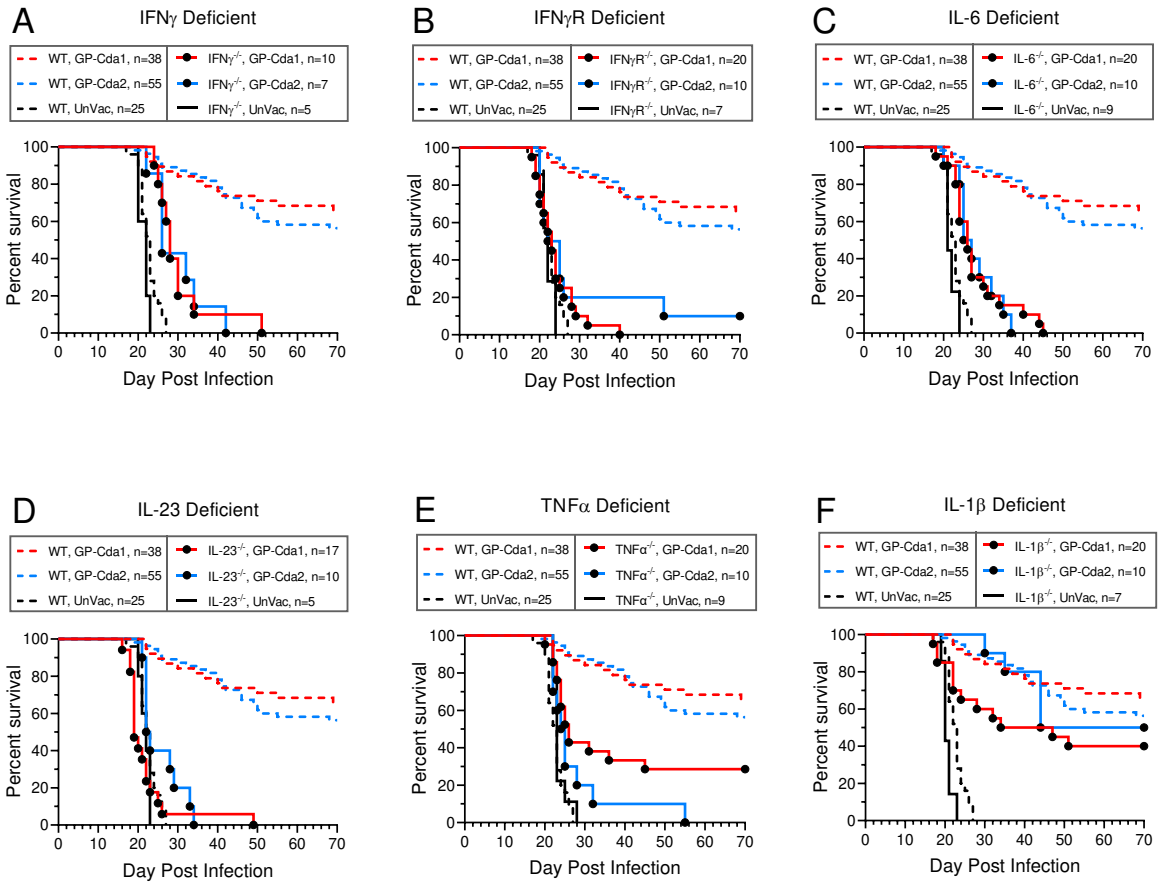

Fig. 7. Effect of host gene deletions in selected cytokines or cytokine receptor on GP-Cda1 or Cda2 vaccine efficacy. Wild-type (WT) mice and mice with selected cytokine or cytokine receptor deficiency (A. IFNɣ$^{-/-}$; B. IFNɣR$^{-/-}$; C. IL-6$^{-/-}$; D. IL-23$^{-/-}$; E. TNFα$^{-/-}$; F. IL-1β$^{-/-}$) received a prime and two biweekly boosts with GP-Cda1 or GP-Cda2. Two weeks after the last boost, mice were challenged with *C. neoformans* and followed 70 days for survival. UnVac = unvaccinated. n denotes the number of mice in the experimental group. All mice were on the C57BL/6 background. Note the same survival curves are shown for WT mice in Fig. 7A to 7F. For Fig. 7A-E, $P<0.001$ comparing survival between knockout and WT mice vaccinated with either GP-Cda1 or GP-Cda2. For Fig. 7F, $P<0.05$ comparing GP-Cda1-vaccinated IL-1β$^{-/-}$ and WT mice.

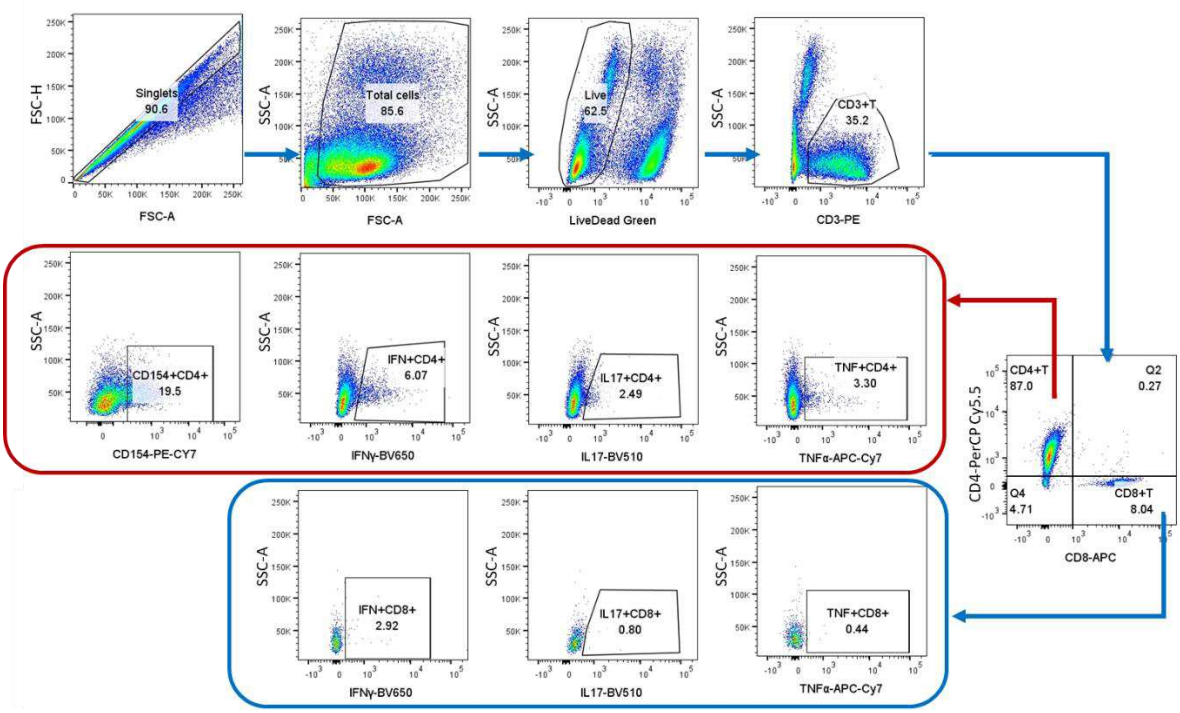

Fig. 1S. Representative flow cytometry plots illustrating the gating strategy for experiments examining T cell activation and intracellular cytokine production in cultured lung leukocytes. Singlet cells were gated based on forward scatter (FSC) height (FSC-H) vs. area (FSC-A). Debris was excluded based on FSC-A and side scatter area (SSC-A). Dead cells were excluded based on LIVE/DEAD green staining. T cells were selected based on $CD3^+$ staining. The $CD4^+CD8^-$ population was selected from the $CD3^+$ population. Finally, the intracellular expression of IFNγ, IL-17A, TNFα and CD154 by the live $CD3^+CD4^+CD8^-$ gated population (shown in red box) was examined. An identical gating strategy was used to examine $CD8^+$ T cells except the $CD4^-CD8^+$ population (shown in blue box) was selected from the $CD3^+$ population. CD154 expression was not analyzed in the $CD4^-CD8^+$ population. The plots are from lung cells of a GP-Cda1/Cda2 vaccinated mouse 10d post infection stimulated *ex vivo* with SEB.

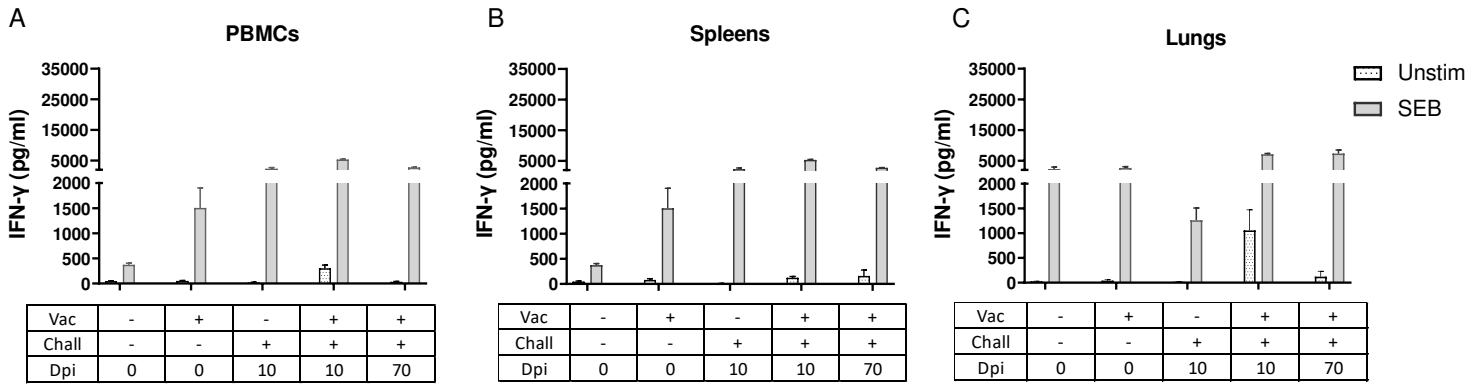

Fig. 2S. IFNɣ production by PBMCs, splenocytes, and lung leukocytes following SEB stimulation. Experiments were designed and conducted as indicated in the Fig. 5 legend. Supernatants of unstimulated (Unstim) or SEB-stimulated PBMCs (A), spleens (B) and lung (C) were collected and analyzed for IFNɣ by ELISA. Each group had 5 mice. Vac, vaccinated with GP-Cda1/Cda2. Chall, challenged with *C. neoformans* strain KN99. Dpi, days post infection. The results of the statistical comparisons between unstimulated and SEB-stimulated groups are shown in Fig. 3S.

A. PBMCs

Group	Unstim vs Cda1		Unstim vs Cda2		Unstim vs KN99		Unstim vs SEB	
Vac- / Chall- / Dpi 0	ns	>0.9999	ns	>0.9999	ns	>0.9999	ns	>0.9999
Vac+ / Chall- / Dpi 0	*	0.0268	****	<0.0001	ns	>0.9999	****	<0.0001
Vac- / Chall+ / Dpi 10	ns	>0.9999	**	0.0061	ns	>0.9999	****	<0.0001
Vac+ / Chall+ / Dpi 10	****	<0.0001	****	<0.0001	**	0.0019	****	<0.0001
Vac+ / Chall+ / Dpi 70	ns	0.7014	ns	0.0769	***	0.0003	****	<0.0001

B. Spleens

Group	Unstim vs Cda1		Unstim vs Cda2		Unstim vs KN99		Unstim vs SEB	
Vac- / Chall- / Dpi 0	ns	>0.9999	ns	>0.9999	ns	>0.9999	****	<0.0001
Vac+ / Chall- / Dpi 0	***	0.0005	****	<0.0001	**	0.0011	****	<0.0001
Vac- / Chall+ / Dpi 10	ns	>0.9999	ns	>0.9999	ns	>0.9999	ns	0.1228
Vac+ / Chall+ / Dpi 10	****	<0.0001	**	0.0034	ns	>0.9999	****	<0.0001
Vac+ / Chall+ / Dpi 70	****	<0.0001	****	<0.0001	****	<0.0001	****	<0.0001

C. Lungs

Group	Unstim vs Cda1		Unstim vs Cda2		Unstim vs KN99		Unstim vs SEB	
Vac- / Chall- / Dpi 0	ns	>0.9999	ns	>0.9999	ns	>0.9999	ns	0.0958
Vac+ / Chall- / Dpi 0	*	0.0186	***	0.0001	ns	>0.9999	**	0.0052
Vac- / Chall+ / Dpi 10	ns	>0.9999	ns	>0.9999	ns	>0.9999	ns	0.4789
Vac+ / Chall+ / Dpi 10	****	<0.0001	****	<0.0001	****	<0.0001	****	<0.0001
Vac+ / Chall+ / Dpi 70	***	0.0001	****	<0.0001	***	0.0004	****	<0.0001

Fig. 3S. Statistical comparisons between groups in Fig. 5 and Fig 2S. Experiments were designed and conducted as indicated in the Fig. 5 and Fig. 2S legends. IFNɣ production of unstimulated cells and cells stimulated with the indicated antigens was compared using two-way ANOVA with Bonferroni's correction. Statistics of comparison were shown in A for PBMCs, B for Spleens and C for Lungs. Vac, vaccinated with GP-Cda1/Cda2. Chall, challenged with *C. neoformans* strain KN99. Dpi, days post infection. Unstim, unstimulated. ns (not significant), $P > 0.05$. *, $P < 0.05$. **, $P < 0.005$. ***, $P < 0.0005$. ****, $P < 0.0001$. Comparisons with statistical differences are shown in red font.

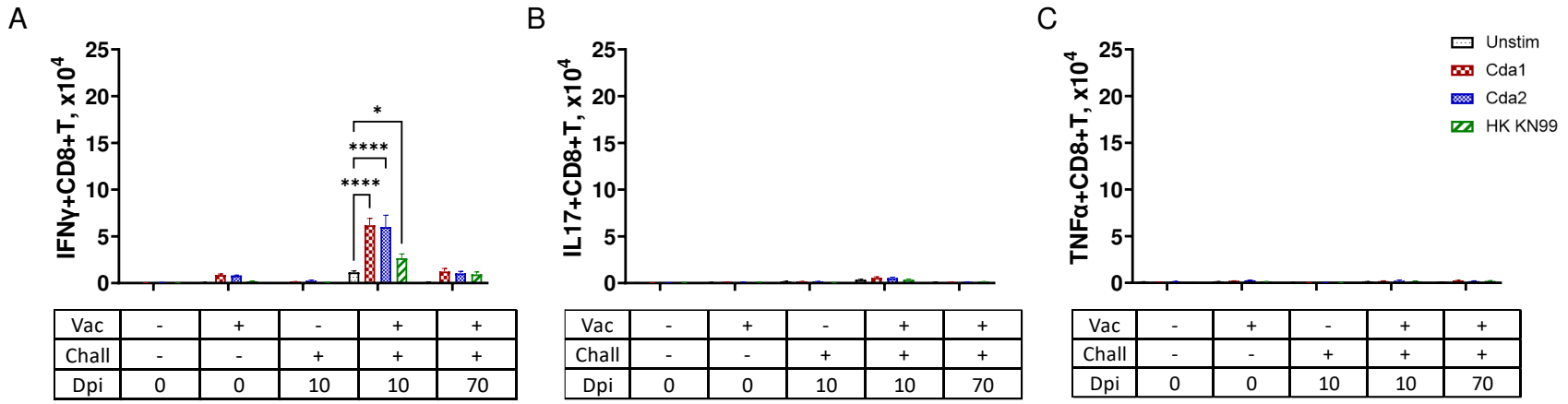

Fig. 4S. Intracellular cytokine production by pulmonary CD8⁺ T cells in GP-Cda1/Cda2-vaccinated and/or infected mice. BALB/c mice were vaccinated thrice at biweekly intervals with GP-Cda1/Cda2. Two weeks after last boost, the mice received a pulmonary challenge with *C. neoformans*. Mice were euthanized at 0 dpi (uninfected), 10 dpi or 70 dpi. Controls included unvaccinated mice euthanized at 0 dpi or 10 dpi. Lungs were harvested and single cell suspensions were prepared. Leukocytes were cultured in complete media supplemented with amphotericin B and stimulated with the indicated antigens or left unstimulated (Unstim) for 18h. Then the cells were collected, stained, and analyzed by polychromatic FACS, as described in Methods. From left to right shows the numbers of lung CD8⁺ T cells producing the intracellular cytokines IFNγ (A), IL-17 (B), and TNFα (C) following *ex vivo* stimulation. Each group had 5 mice. Vac = vaccinated with GP-Cda1/Cda2, Chall = challenged with *C. neoformans*, Dpi = days post infection, HK = heat killed. Two-way ANOVA with Bonferroni's correction was used for comparisons. *, $P<0.05$. ****, $P<0.0001$.

A. CFUs

Group	Summary	*P* Value
Vac- / Chall+ / Dpi 10 vs Vac+ / Chall+ / Dpi 10	ns	0.0952
Vac- / Chall+ / Dpi 10 vs Vac+ / Chall+ / Dpi 70	**	0.0079
Vac+ / Chall+ / Dpi 10 vs Vac+ / Chall+ / Dpi 70	**	0.0079

B. Leukocytes/CD4⁺T/ CD8⁺T cell counts

Group	Leukocytes		CD4⁺T		CD8⁺T	
Vac- / Chall- / Dpi 0 vs Vac- / Chall+ / Dpi 10	ns	0.4785	ns	0.7759	ns	>0.9999
Vac- / Chall- / Dpi 0 vs Vac+ / Chall- / Dpi 0	ns	>0.9999	ns	>0.9999	ns	>0.9999
Vac- / Chall- / Dpi 0 vs Vac+ / Chall+ / Dpi 70	ns	>0.9999	ns	>0.9999	ns	>0.9999
Vac- / Chall- / Dpi 0 vs Vac+ / Chall+ / Dpi 10	****	<0.0001	****	<0.0001	***	0.0002
Vac- / Chall+ / Dpi 10 vs Vac+ / Chall+ / Dpi 10	****	<0.0001	****	<0.0001	**	0.0016
Vac+ / Chall- / Dpi 0 vs Vac+ / Chall+ / Dpi 10	****	<0.0001	****	<0.0001	**	0.0011
Vac+ / Chall+ / Dpi 10 vs Vac+ / Chall+ / Dpi	****	<0.0001	****	<0.0001	***	0.0004
Vac+ / Chall- / Dpi 0 vs Vac+ / Chall+ / Dpi 70	ns	>0.9999	ns	>0.9999	ns	>0.9999

C. CD154⁺CD4⁺T

Group	Unstim vs Cda1		Unstim vs Cda2		Unstim vs KN99	
Vac- / Chall- / Dpi 0	ns	>0.9999	ns	>0.9999	ns	>0.9999
Vac+ / Chall- / Dpi 0	ns	>0.9999	ns	>0.9999	ns	>0.9999
Vac- / Chall+ / Dpi 10	ns	>0.9999	ns	>0.9999	ns	>0.9999
Vac+ / Chall+ / Dpi 10	****	<0.0001	****	<0.0001	****	<0.0001
Vac+ / Chall+ / Dpi 70	ns	>0.9999	ns	>0.9999	ns	>0.9999

D. IFNγ⁺CD4⁺T

Group	Unstim vs Cda1		Unstim vs Cda2		Unstim vs KN99	
Vac- / Chall- / Dpi 0	ns	>0.9999	ns	>0.9999	ns	>0.9999
Vac+ / Chall- / Dpi 0	ns	>0.9999	ns	>0.9999	ns	>0.9999
Vac- / Chall+ / Dpi 10	ns	>0.9999	ns	>0.9999	ns	>0.9999
Vac+ / Chall+ / Dpi 10	****	<0.0001	****	<0.0001	****	<0.0001
Vac+ / Chall+ / Dpi 70	ns	>0.9999	ns	>0.9999	ns	>0.9999

E. IL-17⁺CD4⁺T

Group	Unstim vs Cda1		Unstim vs Cda2		Unstim vs KN99	
Vac- / Chall- / Dpi 0	ns	>0.9999	ns	>0.9999	ns	>0.9999
Vac+ / Chall- / Dpi 0	ns	>0.9999	ns	>0.9999	ns	>0.9999
Vac- / Chall+ / Dpi 10	ns	>0.9999	ns	>0.9999	ns	>0.9999
Vac+ / Chall+ / Dpi 10	****	<0.0001	****	<0.0001	****	<0.0001
Vac+ / Chall+ / Dpi 70	ns	>0.9999	ns	>0.9999	ns	>0.9999

F. TNFα⁺CD4⁺T

Group	Unstim vs Cda1		Unstim vs Cda2		Unstim vs KN99	
Vac- / Chall- / Dpi 0	ns	>0.9999	ns	>0.9999	ns	>0.9999
Vac+ / Chall- / Dpi 0	ns	0.1329	ns	>0.9999	ns	>0.9999
Vac- / Chall+ / Dpi 10	ns	>0.9999	ns	>0.9999	ns	>0.9999
Vac+ / Chall+ / Dpi 10	****	<0.0001	****	<0.0001	****	<0.0001
Vac+ / Chall+ / Dpi 70	ns	>0.9999	ns	>0.9999	ns	>0.9999

Fig. 5S. Statistical comparison for lung CFU and cell numbers in Fig. 6. Experiments were designed and conducted as indicated in Fig. 6 legend. Statistics of comparison were shown in (A) for lung CFUs (Man-Whitney test); (B) for lung leukocyte / CD4+T / CD8+T numbers (One-way ANOVA with Bonferroni's correction); (C) for CD154⁺CD4⁺T numbers, (D) for IFNγ⁺CD4⁺T numbers; (E) for IL-17⁺CD4⁺T numbers; and (F) for TNFα⁺CD4⁺T numbers (Two-way ANOVA with Bonferroni's correction were used for C-F). Vac, vaccinated with GP-Cda1/Cda2. Chall, challenged with *C. neoformans* strain KN99. Dpi, days post infection. Unstim, unstimulated. ns (not significant), $P > 0.05$. *, $P < 0.05$. **, $P < 0.005$. ***, $P < 0.0005$. ****, $P < 0.0001$. Comparisons with statistical differences are shown in red font.